GROWTH AND CHARACTERIZATION OF NITROGEN

DOPED NANOCRYSTALLINE

DIAMOND FILMS

Except where reference is made to the work of others, the work described in this thesis is
my own or was done in collaboration with my advisory committee. This thesis does not
include proprietary or classified information.

_____
Maurice Clark

Certificate of Approval:

_____   _____
Thomas A. Baginski   Yonhua Tzeng, Chair
Professor   Professor
Electrical and Computer Engineering Electrical and Computer Engineering

_____   _____
Thaddeus A. Roppel   Stephen L. McFarland
Associate Professor   Dean
Electrical and Computer Engineering Graduate School

GROWTH AND CHARACTERIZATION OF NITROGEN

DOPED NANOCRYSTALLINE

DIAMOND FILMS

Maurice Clark

A Thesis

Submitted to

the Graduate Faculty of

Auburn University

in Partial Fulfillment of the

Requirements for the

Degree of

Master of Science

Auburn University
May 11, 2006

GROWTH OF CHARACTIZATION OF NITROGEN

DOPED NANOCRYSTALLINE

DIAMOND FILMS

Maurice Clark

_____

Signature of Author

_____

Date

VITA

Maurice Clark, son of Herman and Rosie Lee Clark, born in Dothan, Alabama. He graduated from Dothan High School in 1997. Attended Auburn University in Auburn, Alabama and graduated with a Bachelor of Science in Electrical Engineering in August, 2002. He entered Graduate School, Auburn University on September, 2002

THESIS ABSTRACT

GROWTH AND CHARACTERIZATION OF NITROGEN

DOPED NANOCRYSTALLINE

DIAMOND FILMS

Maurice Clark

Masters of Science, May 11, 2006
(B.S., Auburn University, 2002)

79 Typed Pages

Directed by Yonhua Tzeng

Nitrogen doped nanocrystalline (NCD) diamond films have been deposited on a variety of substrates using microwave plasma chemical vapor deposition (MWPCVD). These films have been systematically studied to determine their electrical, emission, and surface properties. The resulting NCD films exhibit increased electrical conductivity with increasing nitrogen concentrations. Electron emission test on these films indicate increasing nitrogen content in the plasma leads to higher emission currents and lower turn on electric fields. The surface roughness of nitrogen doped films also gradually decreases with increasing N_2 content in the plasma. These films have also been studied to determine the effects of microwave power on their properties.

ACKNOWLEDGEMENTS

Style manual or journal used <u>Diamond and Related Materials</u>

Computer software used <u>Microsoft Word   2003</u>

TABLE OF CONTENTS

LIST OF FIGURES

LIST OF TABLES

CHAPTER 1

INTRODUCTION

Considerable research is being performed on diamond because it possesses exceptional mechanical, electrical and optical properties. Diamond is the hardest known material in nature, it is also corrosion resistant with a wide optical transparency window (220 nm and above), in addition diamond has extraordinary thermal properties see Table 1 and 2 for additional properties.

Diamond growth has become a profitable business over the past 10 years. Advances in film quality, growth methods, and polishing make it possible for diamond to compete with existing materials. This progression has been aided by the discovery of nanocrystalline (NCD) and ultrananocrysatlline (UNCD) diamond films. These films are smoother then traditional polycrystalline diamond (PCD), therefore they can be used in applications where PCD diamond films are not suitable. Today diamond films are being using in applications such as thermal management, biosensors, surface acoustic wave devices, cutting tools, optics, microelectronic devices and microelectromechanical MEMS systems.

Several companies such as Delaware Diamond Knives (DDK), P1 Diamond Inc. and Applied Diamond Inc. are currently selling diamond heat sinks and optical grade diamond windows for microwave and infrared frequencies. These films possess thermal and optical properties similar to those of natural diamond.

Table 1.
Properties of Diamond

PROPERTY	VALUE	UNITS
Mechanical hardness	1.0×10^4	Kg/mm^2
Tensile Strength	>1.2	GPa
Compressive Strength	>110	GPa
Coefficient of Friction	0.03	Dimensionless
Sound Velocity	1800	m/s
Density	3.52	g/cm^3
Thermal Conductivity	20	W/cm-K
Thermal Coefficient of Expansion	1.1×10^{-6}	K^{-1}
Debye Temperature	2200	K
Optical Index of Refraction at 591 nm	2.41	Dimensionless
Optical Transmissivity in the far IR	225	Dimensionless

Table 2.
Electrical Properties of Diamond

Property	Value	Units
Dielectric Constant	5.7	Dimensionless
Dielectric Strength	1.0×10^7	V/cm
Electron Mobility	2200	cm^2/Vs
Hole Mobility	1600	cm^2/Vs
Electron Saturation velocity	2.7×10^7	cm/s
Hole Saturation velocity	1.0×10^7	cm/s
Work Function	Negative	On [111] surface
Band gap	5.45	eV
Resistivity	$10^{13}-10^{16}$	ohm-cm

Today diamond is used as a coating on drill bits, reamer and countersinks. Diamond tipped saws are also used to cut nonferrous materials. Additionally, diamond surgerical blades are now use in medical applications e.g. ophthalmology and neural surgery [1]. Figure 1 shows natural and polycrystalline diamond scalpels; these blades are used to make precision cuts and have the capability of integrating optics [1]. Diamond's unique combination of extreme hardness, wear resistance, low coefficient of friction and thermal properties makes it ideal for these applications.

With a thermal conductivity of 25 $Wcm^{-1}K^{-1}$, which exceeds copper by a factor of five, diamond is considered perfect for thermal management purposes. Therefore, diamond is being used as a heat sink for high power devices such as microprocessors, small microwave IC's, laser diodes, detector arrays and microwave tubes. Diamond's high thermal conductivity allows it to uniformly remove heat from devices eliminating hot spots. There are several benefits associated with the use of diamond heat spreaders including increased performance and reliability.

Diamond has better chemical stability then other microelectronic compatible substrates such as gold, glass, silicon and metal oxides therefore it is attractive for biosensing applications. Furthermore, scientists have successfully functionalized diamond films with DNA and proteins using UV photo attachment [2] and thermal decomposition of benzoyl peroxide [3]. Once diamond films have been functionalized they can be used in conjunction with other microelectronic processes to produce biosensor devices.

CVD diamond films are being incorporated into mobile communication devices, television tuners, and optical-communication devices in the form of SAW filters or

a)


```
Acc.V  Spot Magn    Det  WD |                    | 1 mm
10.0 kV 4.0  18x     SE   15.6 T 0001-4  Ph2.5 (T1_4_1)
```
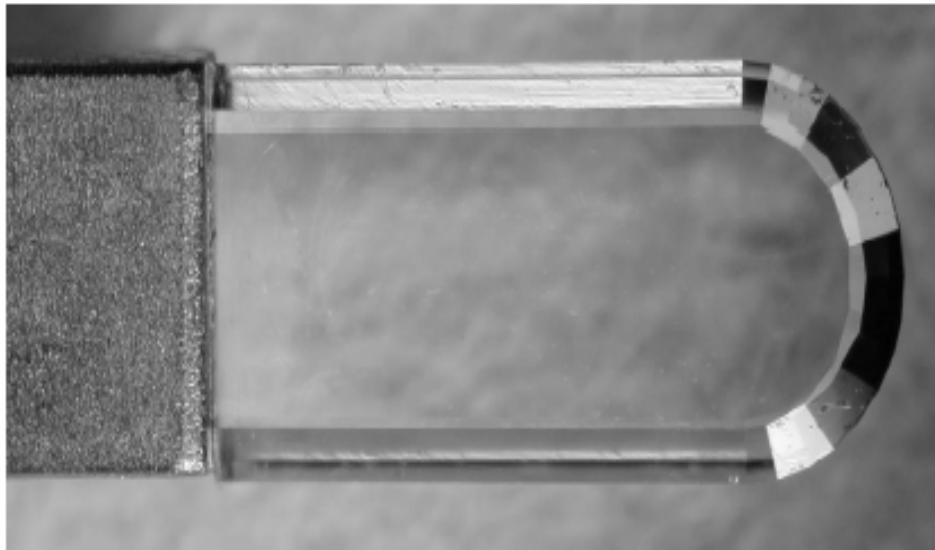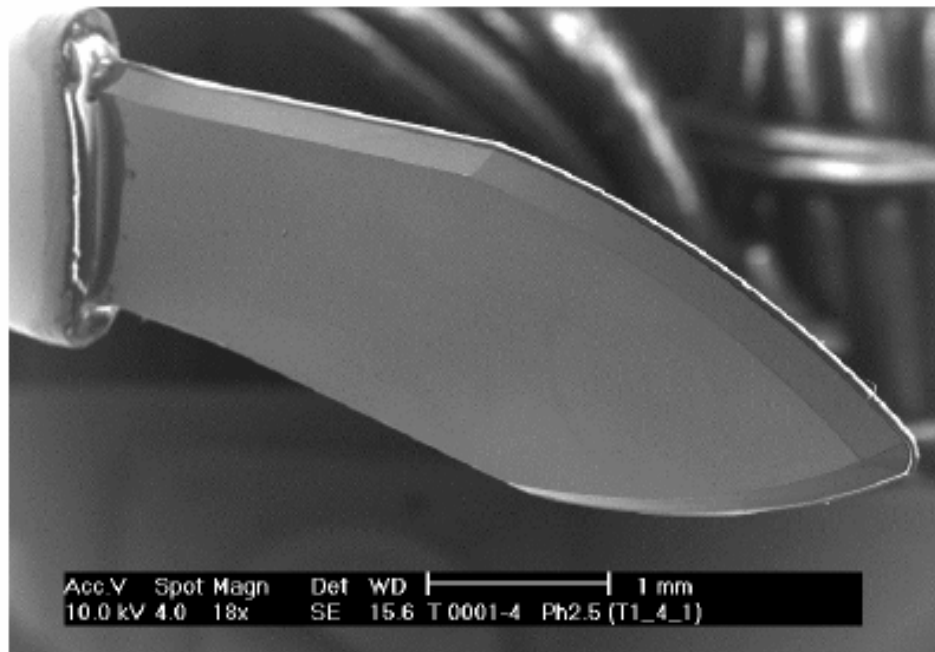
b)

Figure 1. Diamond surgical blades produced from a) natural diamond b) polycrystalline diamond [1]

resonators. Diamond's combination of high elastic constant and high surface acoustic wave velocity (SAW) makes it more desirable then existing materials. Figure 2 shows a schematic of both traditional and diamond SAW filters. These devices are sandwich structures which consist of a piezoelectric layer usually aluminum nitride (AIN) or lithium niobate (LiNbO$_3$), inter-digital transducers IDTs, and finally a diamond layer. These devices convert incoming RF electrical signals into mechanical vibrations (surface acoustic waves) and vise versa. SAW filters with different center frequencies can be constructed by changing the size and spacing of the IDT. The center frequencies of SAW filters is governed by the following relationship $f = v/r$, where v is the phase velocity of the surface acoustic wave and r (electrode width x 4) is equal to the wavelength [4]. These devices are capable of operating at high frequencies. SAW velocities as high as 11,210 m/s have been reported for AIN/ IDT/diamond surface acoustic devices [5].

As mentioned previously, diamond is being used in optical applications. Optical grade diamond lenses, domes and windows are being produced for X-Ray, ultraviolet and infrared frequencies. Diamond's combination of thermal, chemical and optical properties (e.g. its transparency to UV, visible and far infrared bands makes) it ideal for these applications.

Improvements in growth techniques and diamond processing (e.g. polishing, laser cutting etc.) have lead to additional application for diamond thin films. A number of commercial diamond products are now available. Significant research on CVD diamond is still needed to continually increased it's viability as a commercial product.

a)

b)
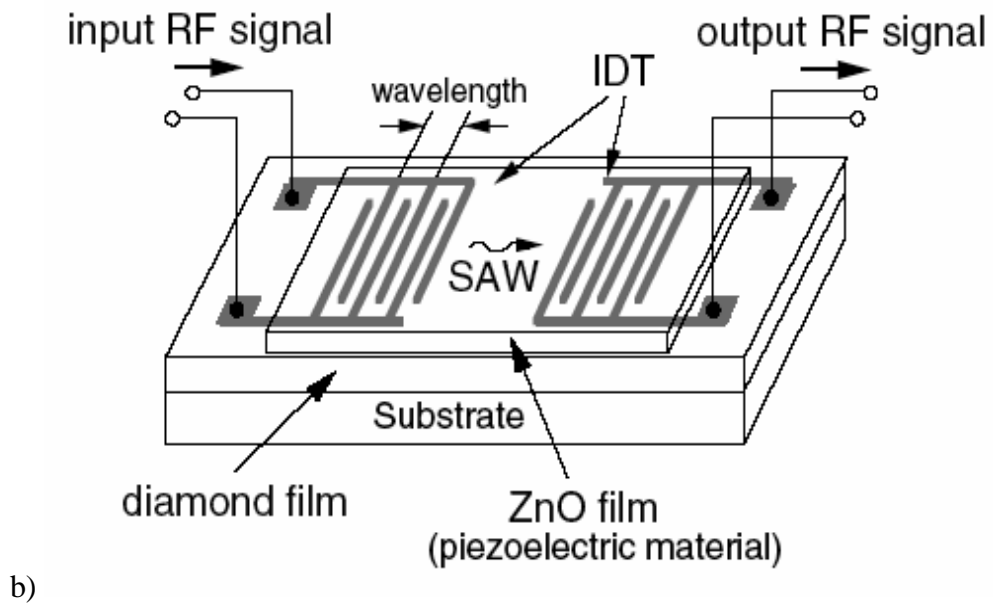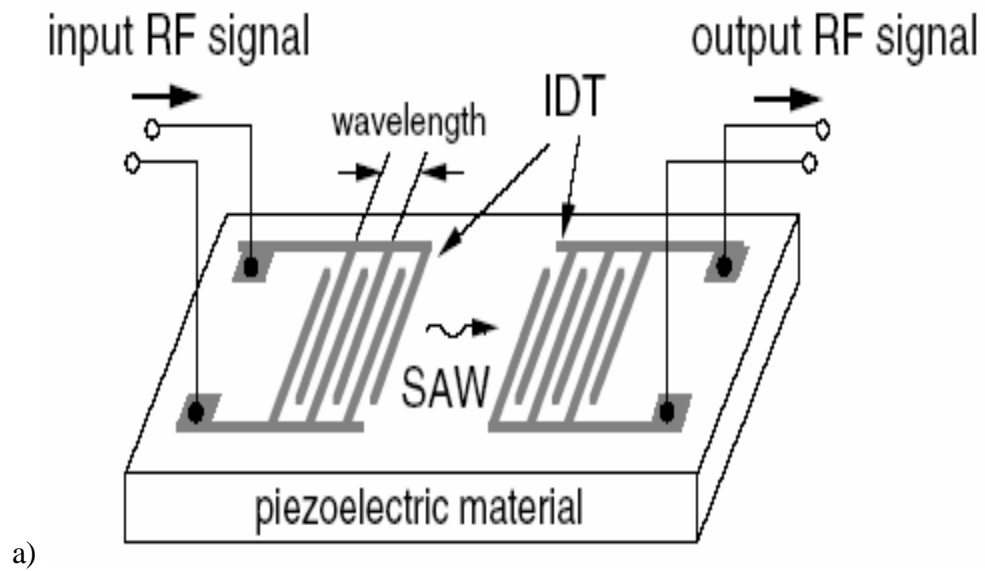
Figure 2. Diagrams of a) Traditional SAW filter b) diamond SAW filter [4]

CHAPTER 2

LITERATURE REVIEW: UNDOPED DIAMOND

2.1 History

The first significant growth of low pressure diamond was achieved by William G. Eversole of the Union Carbide Corporation in 1952 [6, 7] and reproduced by Angus *et al.* in [8, 9] . Eversole and his co-works deposited diamond on pre-existing diamond seeds crystals using a CO/CO_2 gas mixture. This technique yielded diamond films with co-deposits of graphite and diamond, which required a cyclic deposition and removal process. In addition, this method like many of the early methods suffered from low growth rates. Eversole's results predate those of Liander and Bundy on high pressure, high temperature (HPHT) diamond growth [10-11]. His results proved that diamond could be grown at low temperatures and low pressures.

Even with the early success of CVD diamond, it would be many years before significant advancement would take place. The first major breakthroughs came in 1971 when Angus [4] and his co-workers reported the use of atomic hydrogen to remove graphitic deposits during growth. With this knowledge, Vickery of Diamond Squared Industries developed a diamond growth process using a 95%H_2/5% hydrocarbon mixture [12]. Further development followed in 1976 when Russian scientist Deryagin *et al.* [13] reported faceted diamond growth on non-diamond substrates [13]. This was a major step because all previous growth had been done on pre-existing diamond substrates.

8

In 1982 the first high quality diamond films were grown at the National Institute for Research in Inorganic Material (NIRM) by Matsumoto and Setaka [14]. They successfully deposited polycrystalline diamond films using a hot filament reactor. The next year Kamo and others [15] described faceted diamond growth via a microwave plasma reactor. These major advancements spearheaded renewed interest in diamond as an engineering material. Since then many CVD systems and gas mixtures have been use to grow synthetic diamond films.

2.2 Diamond Structure

Diamond is one allotrope of carbon along with graphite, lonsdaleite and fullerenes. All three allotropes consist of hexagonal rings of carbon with different geometries. The hexagonal rings in graphite form flats sheets were as in diamond and lonsdaleite they form puckered chair and boat structures along the <111> direction respectively see Table 3 for a comparison of graphite and diamond properties. The stacking sequence of diamond, lonsdaleite and graphite are ABC, AB, and ABAB respectively [7] see Figure 3. In nature diamond usually forms in the cubic structure, however it can also appear with hexagonal symmetry, this type of diamond is called lonsdaleite and is usually found in meteors. Lonsdaleite is less stable then cubic diamond because its bonds have greater repulsive interaction between next nearest neighbors. Figure 3 shows the cubic diamond structure with a cube edge length of a_o =3.567Å and can be viewed as two interpenetrating FCC structures displaced by (1/4, 1/4, 1/4)a_o along the body diagonal.

Carbon atoms in diamond form a tetrahedral unit where every atom forms strong covalent (sp^3 0.154 nm bond length) bonds with four other carbon atoms at its corners. By virtue of its strong covalent bonding diamond possesses exceptional properties. For

Table 3.
Properties of Diamond and Graphite *(Values taken from)* [16]

Property	Graphite	Diamond	Units
Lattice structure	Hexagonal	Cubic	
Lattice Constant	2.46	3.57	(A) Angstroms
Mohs Hardness	0.5	10	
Thermal Conductivity	30	25	$Wcm^{-1} K^{-1}$
Band gap	-0.04^{1}	5.47	eV
Electron Mobility	20,000	1,800	$cm^2/Vsec$
Hole mobility	15000	1500	$cm^2/Vsec$
Resistivity	50×10^{-6}	10^{20}	Ohm-cm
Dielectric constant low ?	3.0	5.58	
Reflective index (visible)	_	2.4	
Melting point	4450	4500	K
Thermal Expansion	-1.0×10^{-6}	1.0×10^{-6}	K^{-1}
Velocity of sound	2.63×10^{5}	1.96×10^{5}	cm/sec
Highest Raman mode	1582	1332	cm^{-1}

a)

b)

GRAPHITE   LONSDALEITE   DIAMOND

(a)

(b)

(c)

diamond   lonsdaleite

c)
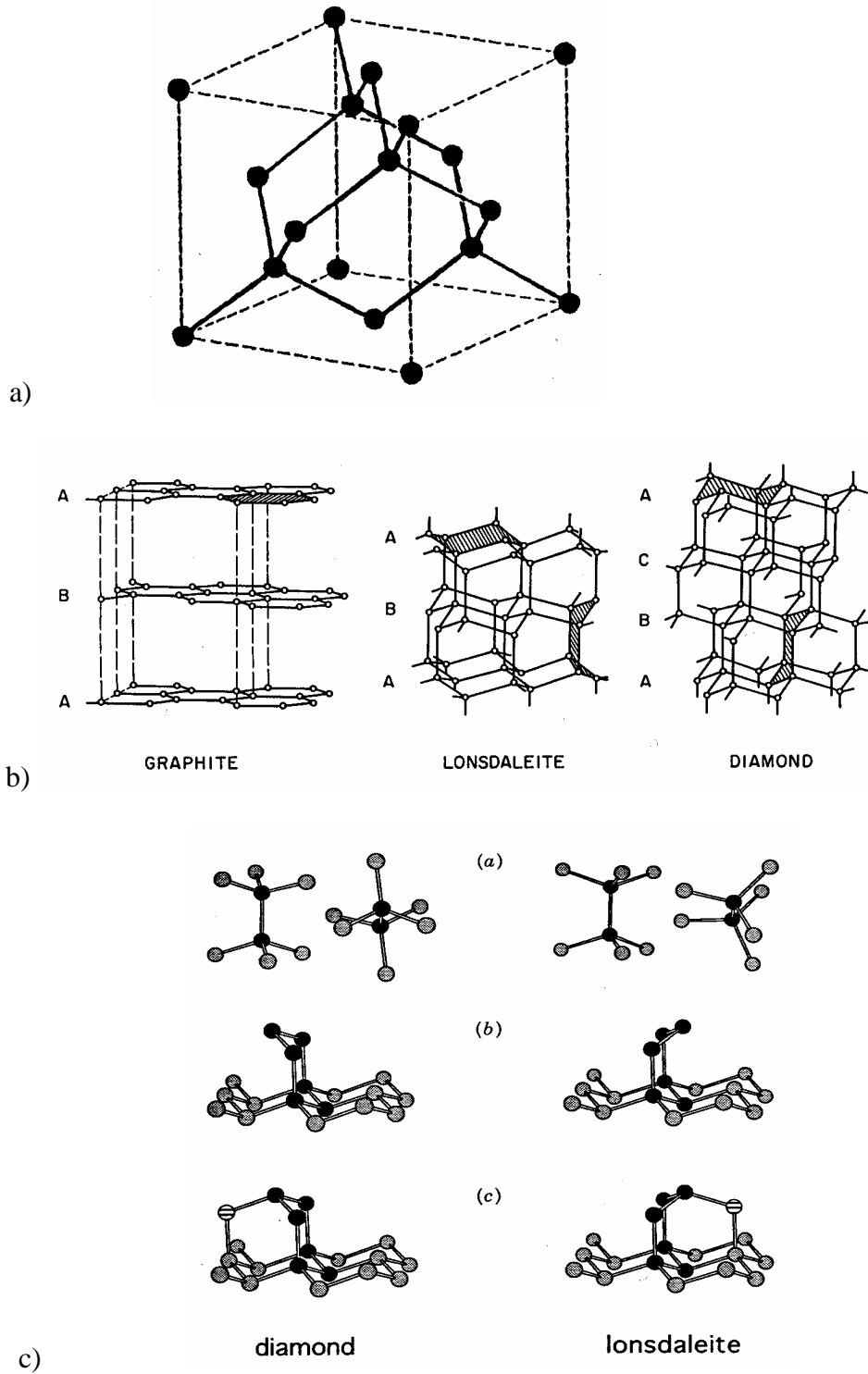
Figure 3. a) Cubic diamond structure [16] b) Diagram of the stacking sequence of graphite, lonsdaleite and diamond along the <111> plane. c) The puckered boat and chair configuration of diamond and lonsdaleite [7]

instance diamond insulating properties are a result of strong bonding between atoms which restricts the amount of electrons available for conduction, most of which are due to defects or impurities in the crystal lattice. Diamond is also the hardest known natural material because of its combination of high atomic density and its three dimensional network or strong covalent bonding. Strong bonding in diamond also allows vibrational energy (heat) to travel through the crystal lattice rapidly, as a result diamond has excellent thermal properties.

2.3 Chemical Vapor Deposited (CVD) Diamond

CVD diamond films grow under conditions where graphite is the stable form of crystalline carbon. Therefore CVD systems must create an environment where diamond growth is favored over graphite deposition. A variety of methods have been used to deposit CVD diamond. However, they all have three things in common. First, all CVD systems have some way to activate reactant gases, whether it is by thermal, electrical or combustion methods. Secondly a carbon source is needed to extend the diamond lattice. Finally, condition in the system must be such that diamond growth is encouraged while graphite formation is suppressed.

CVD diamond growth occurs at pressures of 0.1 Torr and atmospheric pressure. The substrate temperature during growth is usually between 400°C and 1000°C. Various precursor gases have been used in combination with hydrogen to grow CVD diamond films including methane [17], alcohols [18-19], carbon monoxide [20] and carbon dioxide and halides [21-23]. For these reactions hydrogen plays several significant roles; first hydrogen abstraction creates vacant surface sites were radicals such as CH_3 can bond

secondly it prevents graphitization of the surface by terminating dangling carbon bonds and finally atomic hydrogen etches graphite at a much faster rate then diamond.

The growth mechanism for diamond in excess hydrogen has been the subject of much debate, but it is generally accepted that CH_3 is the growth species. Figure 4 depicts CH_3 insertion into the diamond lattice via hydrogen abstraction reactions. In this process the surface is initially covered with hydrogen, however hydrogen abstraction creates vacant sites where CH_3 can chemosorb on the surface. If the adjacent carbon site undergoes the same process with an additional hydrogen abstraction then the resulting CH_2 radical will react with the CH_3 radical completing the ring. This is just one possible mechanism for CH_3 insertion into the diamond lattice [24].

Hydrogen depleted gas chemistries have also been studied. In fact Gruen and his co-workers at Argonne National Labs reported the growth of ultrananocrystalline diamond (UNCD) using CH_4 [25] or C_{60} [26-27] diluted in Ar. The resulting diamond films were extremely smooth with small grain sizes of 3 to 5 nm. N_2/CH_4 plasmas have also been used to grow diamond films. Wu *et al.* [28] reported growth of smooth diamond films with a grain size of 10 nm. Xu *et al.* [29] also reported similar results with grains sizes ranging from 10 to 100 nm. It should be noted that both Wu and Xu applied a negative bias (-90V) to the substrate during growth. These results demonstrate that hydrogen is not absolutely necessary for diamond growth. The growth mechanism for CVD diamond films grown under the above conditions is believed to be C_2 dimers which increase for this type of gas chemistry.
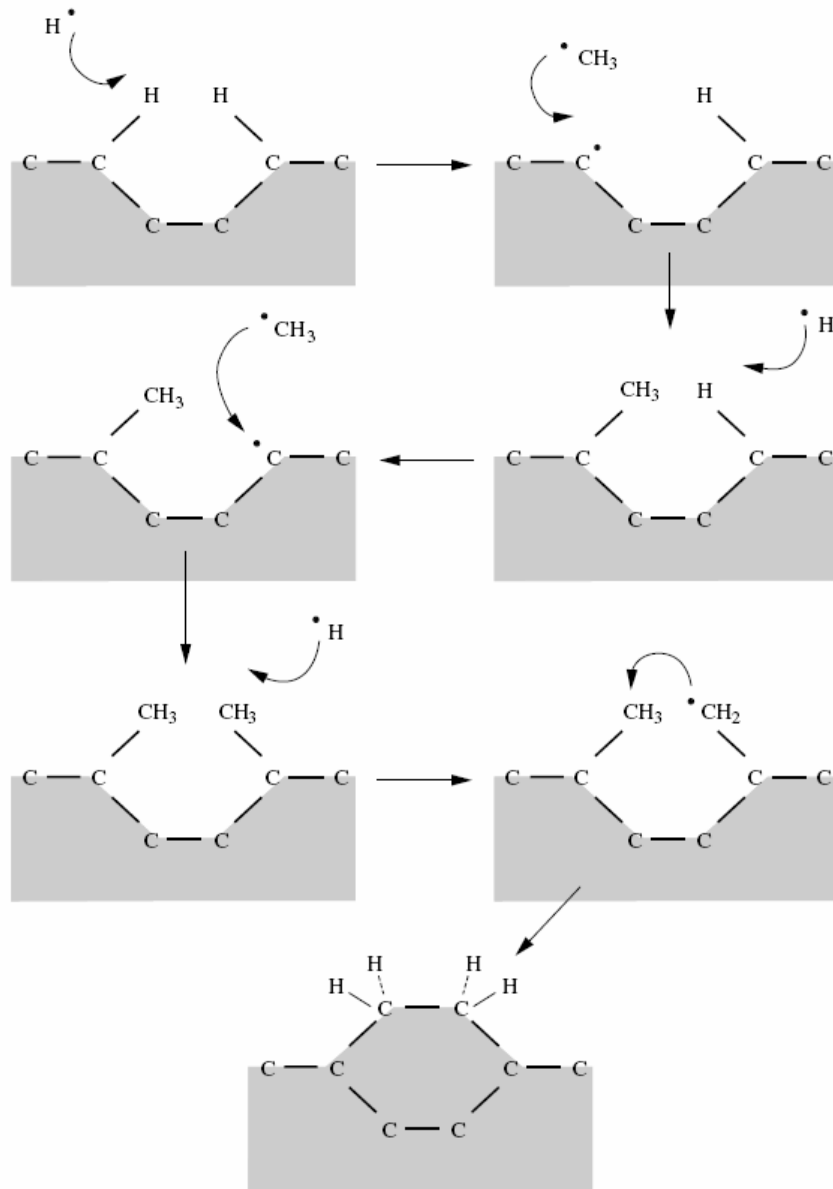
Figure 4. Diamond growth via CH$_3$ insertion into the diamond lattice [24]

2.4 CVD Diamond Growth Methods

Figure 5 depicts a typical microwave plasma CVD (MPCVD) system. MPCVD employs a plasma discharge to activate gas reactants. Microwave energy is supplied to gas phase electrons which transfer their energy through collisions with ions and gas molecules to generate reactive species such as C_2, CH_3, C_2H_2 etc. These species interact with the substrate an eventually form a diamond film. MPCVD is one of the most popular methods for diamond deposition. This method permits reliable and reproducible phase pure diamond growth. Moreover, this type of system allows a variety of gas reactants to be used some of which may be detrimental to other systems e.g. halogens. The main drawback of this type of system is the high equipment cost.

Another popular diamond growth technique is hot filament CVD (HFCVD). A typical HFCVD system shown in Figure 6 is composed of an evacuated chamber where a metal filament such as tungsten, rhenium, or other refractory metal is heated to temperatures between 2000°C and 2300°C. The heated filament dissociates reactant gases creating reactive precursors such as C_2, CH_3 and CH_2 which impinge on the substrate to form a diamond films. This type of diamond growth is very attractive because of its low cost and simplicity. It is also good for deposition of large areas and for depositing diamond on three-dimensional substrates. Drawbacks of a HFCVD system include filament contamination and a limited deposition time.

Diamond growth via a dc-arc jet system was first reported by Kuriharra in 1988 [31]. DC arc discharges utilize an electric discharge (arc) to partially dissociated reactant gases. This system usually consists of two chambers one where the gas is partially
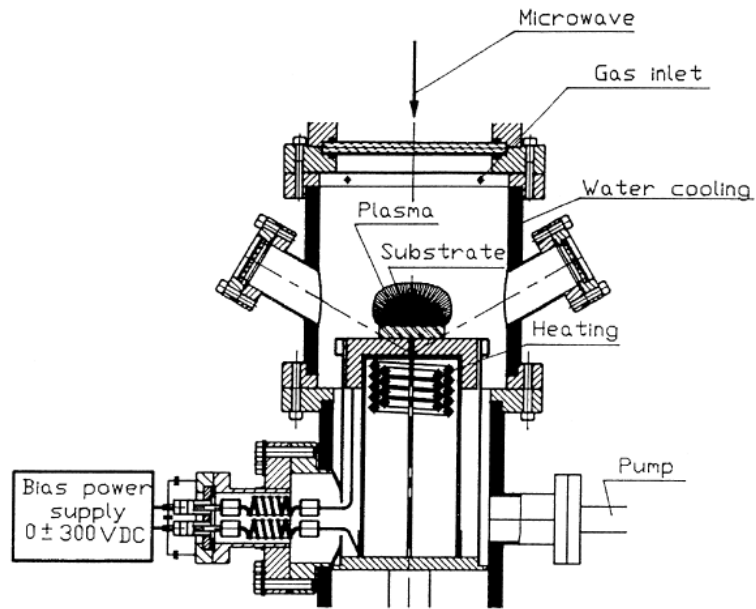
Figure 5. Microwave CVD System [30]
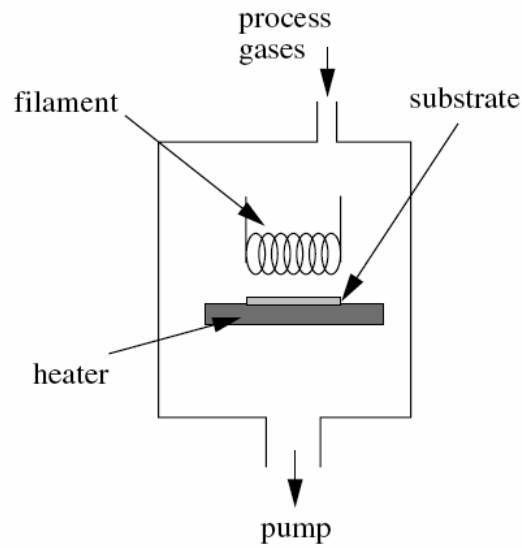
Figure 6. Hot Filament CVD Reactor [24]

dissociated and another where the gas expands through a small nozzle to impinge on the surface of the substrate. One of the most popular designs consists of a concentric cathode and a surrounding cylindrical anode see Figure 7. Arc discharges exhibit fast growth rates but are usually limited to small deposition areas. The major drawback of this type of system is the high temperatures $T_s \sim 1000°C$ - $1500°C$ experienced by the substrate during growth.

Figure 8 is a schematic of a direct current plasma assisted CVD (DC-PACVD). In this type of system, plasma is generated by applying a voltage between two electrodes called the anode and cathode. The substrate is usually placed on the anode to encourage diamond growth. Gas activation is similar to MPCVD where energetic electrons generate reactive species through collisions with ions and gas reactants.

Combustion flame assisted CVD diamond growth via a commercial plasma torch was first reported by Hirose in [32]. This technique employs an oxyacetylene flame for combustion synthesis of diamond. The combustion flame consists of a primary combustion zone where reactant gases C_2H_2 and O_2 are consumed to produce CO and H_2 as well as other reactive species which pass through the intermediate and outer diffusion zone where they are deposited on the substrate. This method allows high pressure diamond growth with relatively high growth rates. Just as with the dc arc-jet the combustion flame method suffers from high substrate temperatures. Figure 9 shows an oxyacetylene combustion system.

A radio frequency plasma CVD is depicted in Figure 10. High voltage coils generate RF waves which excite the plasma. This type of plasma is called a hot plasma because the electrons and heavier ions both gain energy from the changing electric field and

17
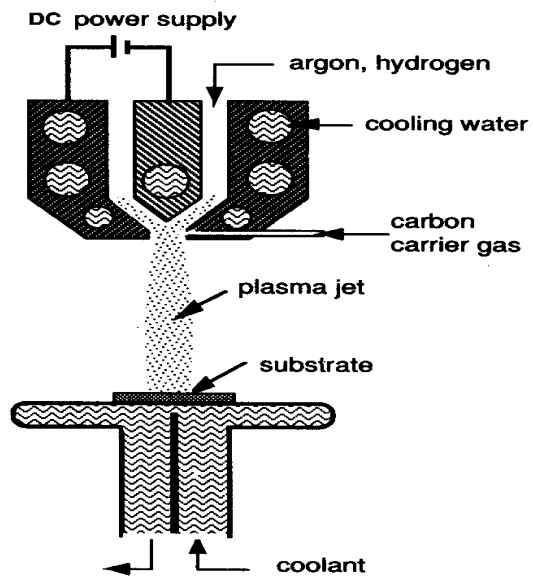
Figure 7. D. C. Plasma Jet [6]
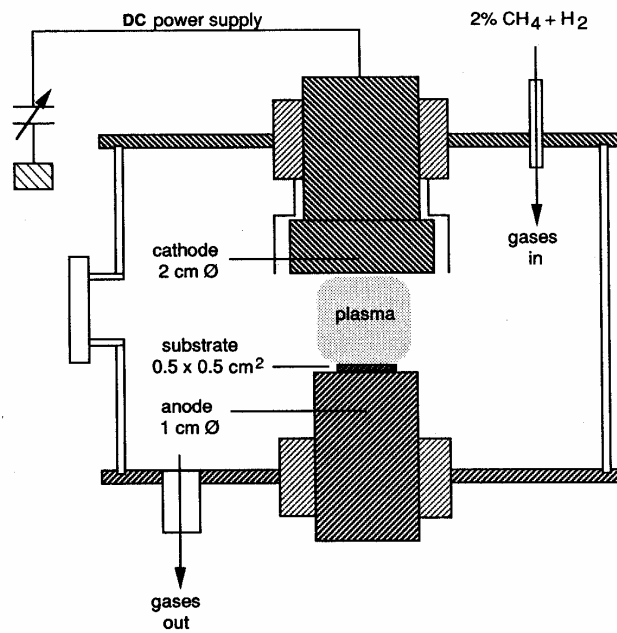
Figure 8. D. C. Plasma System [6]
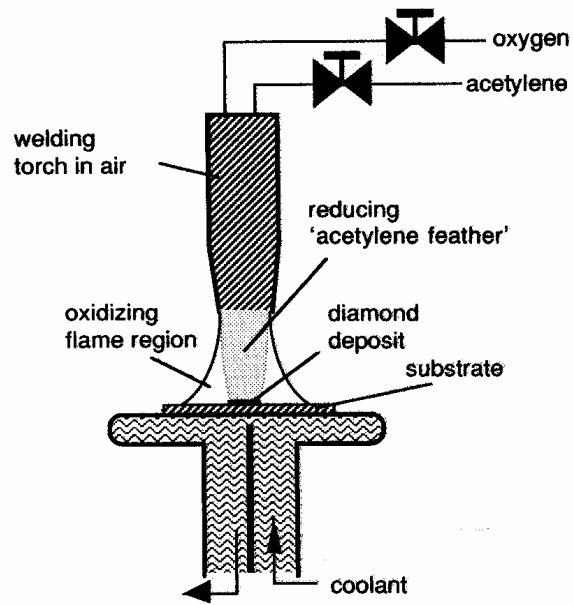
Figure 9. Combustion Flame CVD schematic [6]
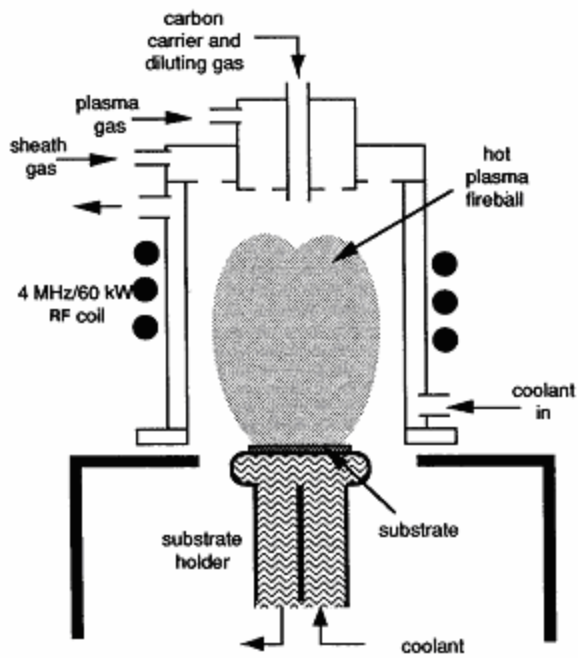
Figure 10. RF Plasma Reactor [1]

transfer their energy to molecules, radicals and to the chamber wall causing the gas temperature in the hot zone to be >5000°C for high pressure growth. Growth rates as high as 30 to180 um h^1 have been reported for this type of deposition. However, this type of growth requires large amount of gas reactants, and low pressure deposition usually leads the formation of diamond-like carbon (DLC).

2.5 Crystallinity of CVD Diamond Films

The crystallinity of diamond is important because it affects the specific characteristics of diamond films. These films are separated into four categories, single crystal, polycrystalline, nanocrystalline and ultrananocrystalline diamond. Each form of diamond has characteristics which makes it suitable for specific application, for instance ultrananocrystalline diamond films have low surface roughness, no staction and their electrical properties are tunable therefore they are suitable for micro electrochemical MEMS applications.

2.5.1. Single crystal diamond

CVD single crystal diamond films have historically been grown on natural and HPHT (homoepitaxial growth) diamond substrates. These diamond films were originally hampered by low growth rates; however improvements in growth conditions have lead to increasing growth rates. Researchers like, Yan *et al.* [35] have reported high growth rates up to 150 um-h^{-1} on HPHT diamond films using a high powered MPCVD reactor. This is important because almost all single crystal diamond films are grown using this type of process.

Now it is also possible to grow single crystal diamond films on non-diamond (heteroepitaxial growth) substrates. Heteroepitaxial growth of single crystal diamond is

usually achieved by growing diamond films on metal oxide/Iridium layers. Bednarski *et al.* [33] study diamond growth on (001) SrTiO$_3$ plates with a Ir (001) epitaxial layer using MPCVD. The resulting films formed a featureless diamond slab with cleaved (111) planes along the <110> directions, similar to natural diamond. Other methods for growing single crystal diamond include growing oriented diamond films on substrates such as c-BN. Yoshikawa in [34] used Raman and X-ray diffraction techniques to determine the orientation of diamond films grown on c-BN substrates using DC plasma. His results revealed that diamond's crystallographic orientation was almost the same as the (111) c-BN. These results are encouraging, however this type of growth is problematic because of the numerous steps required to prepare substrates for diamond deposition. Better substrate materials for heteroepitaxial growth of SCD are needed to make it feasible.

2.5.2. Polycrystalline Diamond

Another form of diamond is polycrystalline diamond (PCD). These films are characterized by well faceted random grains 100 to 1000 nm in length with shared axis or planes (twinning) as shown in Figure 11. PCD films retain many of the extraordinary properties of natural diamond.

These films are traditionally grown using methane/hydrogen plasma (1%CH$_4$/99%H$_2$). PCD growth involves competitive growth of diamond crystallites, where crystallites with the highest growth normal to the surface envelop slower growing crystals. This type of growth leads to increased grain size with increasing thickness (van der draft). Another feature of PCD is the fact that its morphology and orientation can be tuned by controlling the a parameter which is defined by the following equation:

21
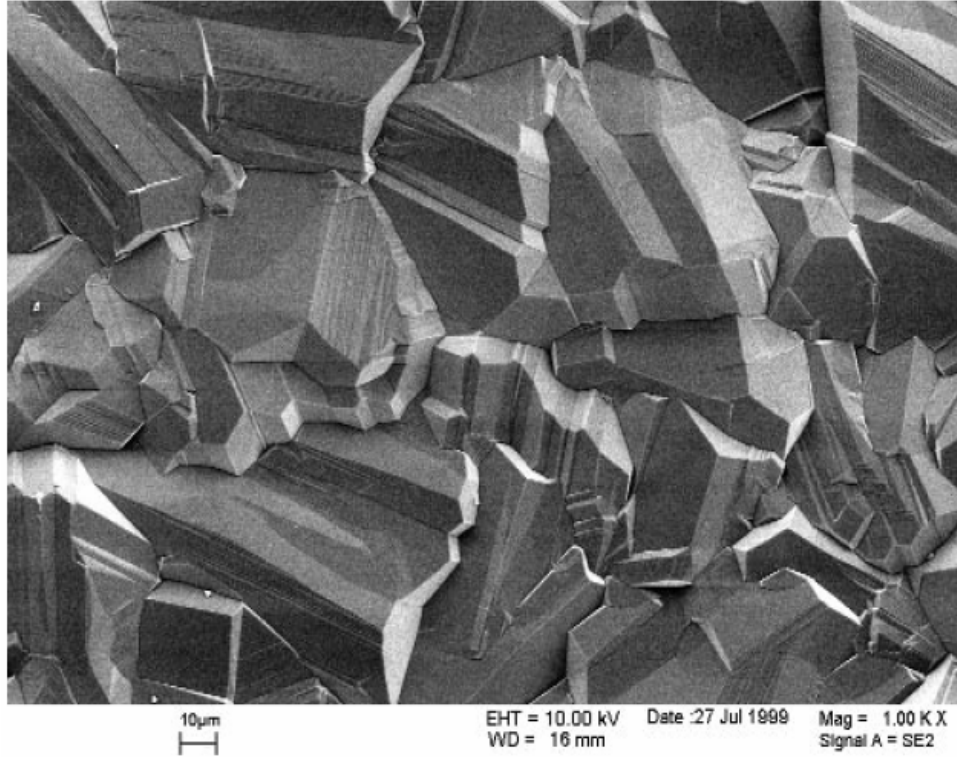
Figure 11. SEM image of a polycrystalline diamond film. [40]

$$a = \sqrt{3}\frac{v_{100}}{v_{111}},$$

,where v_{100} and v_{111} represent the growth velocity in the (100) and (111) direction, when a is equal to 1 then single crystal diamond forms, a equal to 3 results in cubes and finally a between 1 and 3 leads to cubo-octahedra diamond [36] as shown in Figure 12. The a parameter can be easily controlled by changing growth parameters such as power, pressure etc.

PCD films are being used in optical applications. Ultra-thin freestanding X-ray windows made from PCD films have been described by Ying *et al.* in [38]. These windows have excellent transmissivity in the soft X-ray range. Near infrared antireflective filter windows have also been produced by Ying *et al.* [37]. These windows
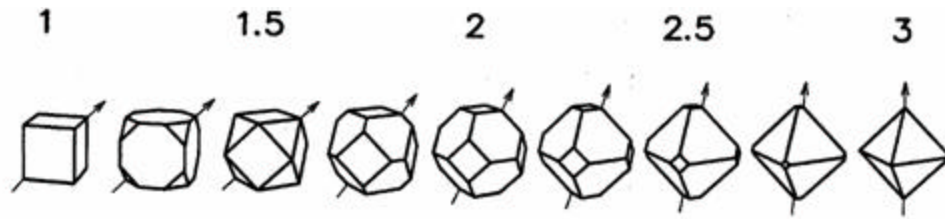
Figure 12. The shapes associated with different a values between 1 and 3 for PCD. [37]

have been successfully used in on-line monitoring at Shanghai Baosteel Works and they produce an annual benefit of 2.4 million RMB Yuan. Additionally, optical CVD diamond lenses with thermal conductivity of 20.8 $Wcm^{-1}K^{-1}$ have been reported by Woerner *et al.* in [39]. PCD diamond lenses were fabricated by growing diamond on Si substrates with spherical impressions.

Improvement in polishing techniques and growth quality has extended the number of application for which PCD diamond films are suitable. Even though PCD diamond films can be polished and used in many applications, it is still necessary that smoother forms of diamond thin films be developed to take full advantage of diamond microelectronic devices.

2.5.3. Nanocrystalline Diamond

These films consist of ballas (cauliflower) like structures with grain sizes 50 -100 nm. Figure 13 shows two different NCD diamond films. Nanocrystalline diamond films exhibits improve surface roughness, reduced grain size, and increased mechanical strength as compared to PCD.

Nanocrystalline films have been grown using a variety of procedures. One of the most popular ways to grow NCD involves replacing H_2 with a noble gas such as Ar or He. Lin *et al.* in [41] reported the transformation of microcrystalline diamond to
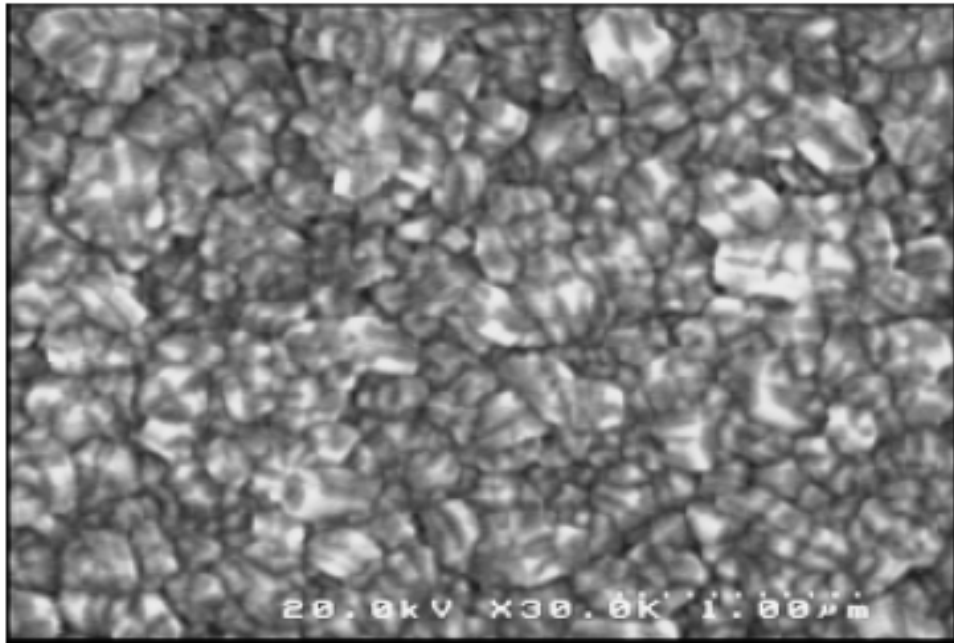
a)
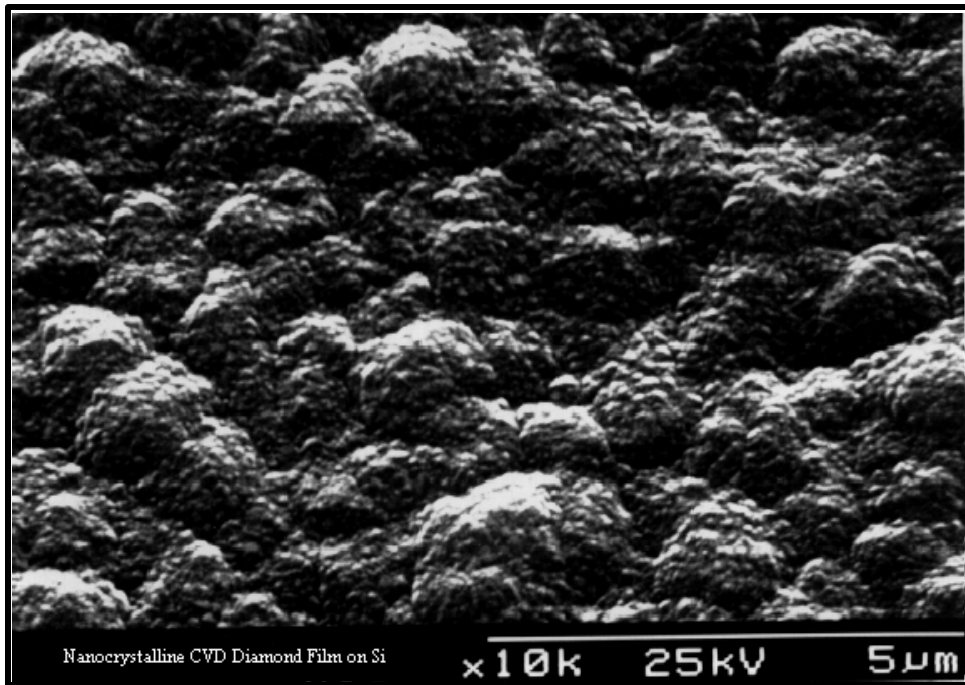
b)

Figure 13. SEM images of NCD grown using a 2 step bias growth process [24] b) NCD film grown using CH$_4$/H$_2$ [45]

24

nanocrystalline diamond with the addition of >95.5% Ar to conventional CH_4/H_2 mixtures. Similar results are reported by Jones *et al*. in [42] using a hot filament reactor (transformation of microcrystalline to nanocrystalline occurred with >90% Ar and He addition). Biased enhanced growth is another process for growing NCD diamond films. Sharda *et al*. in [43] described growth of NCD via bias enhanced growth, with 5% CH_4 in hydrogen; this growth chemistry results in NCD films with rms surface roughness of 17 nm. Gu [44] reported similar result with ion bombardment of different energies, nanocrystalline diamond films appeared with a bias voltage over 120V.

NCD films exhibit superior structural properties with fracture strength and elastics modulus of 4.0 GPa and 1020 GPa respectively [45]. In addition these films have low intrinsic vertical and horizontal stress; therefore freestanding diamond cantilevers show no detectable bending, which makes them suitable for sensor and MEMS applications [45].

Extensive study of NCD diamond films is being conducted to determine its electron emission properties. Low emitting NCD films have been reported by several authors. Wu et al. [28] used MPCVD to grow low emitting NCD films using CH_4 and N_2 precursor gases. The resulting diamond films have low turn on voltages which decrease from 4.9 V/um to 1.3 V/um when the CH_4/N_2 flow ratio is decreased from 5.6 to 1.4%. These low emitting diamond films also have good long term current stability with a maximum emission current of 10 mA. Similar results were reported by Xu in [29]. Subramanian *et al*. [46] used MPCVD to grow a NCD film with a low turn on voltage of 7 V/um using $CH_4/H_2/N_2$ plasma. These results indicate that NCD diamond is suitable for electron emission applications.

2.5.4. Ultrananocrystalline Diamond

Ultrananocrystalline (UNCD) diamond films are grown via argon rich microwave plasmas with either C_{60} [26, 27] or CH_4 [25] as the carbon source. Extensive characterizations reveal that UNCD films are phrase pure diamond with 3-5 nm grains, which are atomically abrupt with high-energy grain boundaries. Thin UNCD diamond films less 100 nm thick demonstrate properties, which are equal to and in some cases superior to natural diamond. Figure 14 shows an SEM image of a UNCD films grown using a hot filament reactor.

UNCD films are being considered for use in biosensor or bio-modification applications. In [47] Yang *et al.* used photochemical attachment along with other processes to covalently link DNA to UNCD films. Functionalized diamond films can be used with existing microelectronic fabrication processes to create a biosensor device. UNCD is also being studied for use in microelectro-mechanical systems MEMS. In [48] Auciello and his colleagues demonstrated that UNCD MEMS devices can be fabricated using a combination of Si and diamond fabrication processes. In addition, Espinosa *et al.* [49] conducted micro cantilever deflection and membrane deflection experiments, which showed that UNCD films possess mechanical properties that make it ideal for MEMS devices i.e., elastic modulus values of 930-970 GPa and fracture strength in the range of 5.05 GPa

The growth precursor for UNCD films is believed to be C_2 carbon dimmers. Carbon dimmers are easily detected in Ar/CH_4 plasmas by optical emission spectroscopy (OES) and absorption spectroscopy [50]. Reactions between C_2 and diamond have been studied on both hydrogen terminated and non-hydrogen terminated diamond films.

26

Figure 14. Scanning electron microscopy of UNCD [45]

Horner *et al.* [50] concluded that reactions between dicarbon C_2 and the (110) hydrogenated diamond surface are energetically favorable with a small activation barrier; similar results have been attained by Sternberg *et al* in [52] and Redfern *et al.* in [51] on hydrogen free (100) and (110) diamond. Sternberg reported that diamond growth from gaseous dicarbon could occur via direct absorption on clean sites or the migration of dicarbon on top of existing C_{2n} chains. Sternberg *et al.* in [53] also used high density tight bonding and showed there are additional pathways for growth on the (100) non-hydrogenated diamond (100)x(2x1) surface; these pathways were found to have higher energy barriers then those on the hydrogenated (110) plane. Even though there is a lot of evidence for C_2 as the main growth species for UNCD, it should be noted that there is still ~1% H_2 in the plasma which means there are possibly other species such as H^+, CH_3, C_2H, C_2H_2 which could be participating in the growth process [54]. The extent of their participation needs to be resolved.

Figure 15 demonstrates one possible mechanism for C_2 incorporation which was proposed by Horner and Redfern *et al.* [50-51] it involves C_2 insertion into a (110) hydrogen terminated diamond surface. First C_2 inserts itself into C-H bonds then C_2 rotates so that it can insert itself into the C-H bond across from it. The next two steps involve repeating steps 1 and 2. The final step requires restoration of the (110) plane with the formation of a bond between the carbon atoms in the adjacent surface dimmers.

2.6 CVD Nucleation

Conventional heteroepitaxial CVD growth requires a significant incubation period before diamond growth commences. Therefore most CVD films are grown via a pretreatment process such as substrate scratching, diamond seeding or biasing.

28
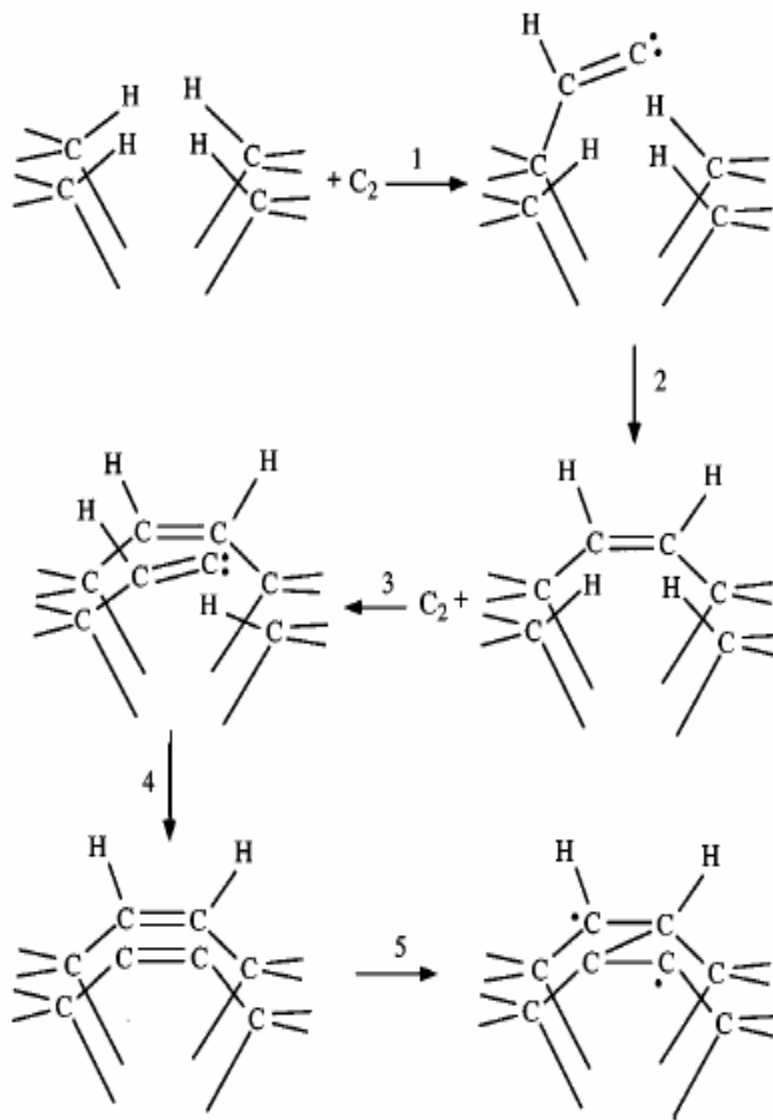
Figure 15. Possible Mechanism for C_2 insertion into the diamond lattice [50]

Pretreatment provides the substrate with diamond nuclei to initialize diamond growth under the right conditions. The nucleation density affects the microstructure, morphology, homogeneity, defect formation, and adhesion of diamond films [55]. For instance, the higher the nucleation density the shorter the coalesce time which results in reduced surface roughness.

A well accepted nucleation method involves mechanically polishing the substrate with abrasives such as SiC [56], c-BN [57], Al_2O_3 [58], ZrB_2 [59], Cu [60], and diamond [61-62]. Several mechanisms have been proposed to account for the enhanced nucleation density of polished substrates; including the seeding effect were diamond residue from polishing material provide the growth template for homoepitaxial diamond growth; the creation of high-energy sites or chemically active sites; and finally; the removal of surface oxides. Nucleation densities for scratched substrates can range from 10^6-10^{10} cm^{-1}. Unforturely, this type of pretreatment results in damage to the substrate and therefore is not suitable for applications, which require a smooth surface. Another fault of this method is the fact that 3-D objects can not be nucleated in this manner.

Another popular nucleation method is ultrasonic agitation which was first reported by Hirakuri [63]. This process involves ultrasonically agitating the substrate in a nanodiamond solution such as nanodiamond powder and methanol. Ultrasonic agitation gives a homogeneous scratching of the substrate surface by nanodiamond powder. Ultrasonic agitation yields a nucleation density between 10^7 and 10^{11} cm^{-1}. This process is less destructive and provides a more uniform nucleation compared to mechanical polishing.

Micro-diamond seeding is another nucleation method which gives a nucleation density around 10^8-10^9 cm^{-1}. Seeding is accomplished by electrophoresis or by dipping, spinning or spraying the substrate with a microdiamond solution. With this method the micro diamond seeds on the substrate serve as nucleation sites for diamond growth. This process suffers from agglomeration of diamond nanoparticles and surface contaminations.

One of the most effective nucleation processes is bias enhanced nucleation. BEN involves placing a voltage across the substrate under either growth conditions or slightly different conditions for short periods usually 30 minutes to 1hr [64-65]. This method utilizes ion or electron bombardment to remove native oxides; it also suppresses oxide growth and creates substrate defects to promote growth of a small diamond layer; which serve as the seeds (growth sites) for further homoexpitaxial growth. BEN has been accomplished in both MPCVD and hot filament CVD systems [64-65]. This process is suitable for application where smooth and clean surfaces are required. Nucleation density of 10^9-10^{10} cm^{-1} has been achieved.

Other nucleation methods have been studied including surface coating of DLC [66-67], carbon layers [68] and hydrocarbon oil [69]. In [69] Morrish reported enhanced nucleation on diamond scratched substrates which were subsequently smeared with oil (oil smeared samples produced almost continuous, pinhole free films). Morrish also discovered that the formation of a carbide layer was not necessary to produce the effects of enhanced nucleation. Instead he and his colleague concluded that the prevention of carbon diffusion into the bulk substrate material results in enhanced nucleation.

2.7 CVD Diamond Substrates

Choosing the appropriate substrate for CVD deposition is critical because of the extreme conditions of CVD growth. Three major factor must be considered when choosing a substrate material 1) it must have a high melting point to withstand the temperature of CVD diamond growth 2) substrates must have low index mismatches and 3) the coefficient of thermal expansion must be close to diamond to ensure good adhesion. To date silicon is the most used substrate because of its properties, availability and low cost. In addition researchers have discovered that substrates which react with carbon or form carbide layers have a lower incubation period then substrates which do not.

Studies by Joffereau [70] and Lindlbauer [71] reveal that a carbide layer forms on substrates such as silicon before diamond growth commences. Lux and Hauber indicate that substrates that formed carbide layers the fastest had the shortest incubation period [72]. They also proposed that carbon dissolves into the substrates which results in stable carbide layer. Diamond nucleation occurs when the carbon concentrations on the surface reaches its saturation point.

Therefore, materials such as Cu, Sn, Pb, Ag and Au which and do not form a carbide layers and have little or no solubility in carbon can be used to make freestanding diamond films because diamond does adhere well to these substrates. On the other hands materials like Pt, Pd, Rh, Ni, Ti, and Fe, which react readily with carbon, are not useful because carbon will be absorbed into the bulk material which could cause a long incubation period and affect the physical properties of the material.

CHAPTER 3

LITERATURE REVIEW : CONDUCTIVE DIAMOND FILMS

3.1 Conductivity of Diamond Films

At room temperature, diamond is a good electrical insulator with a resistivity of approximately 10^{16} ohm-cm. The conductivity of diamond can be modified by hydrogen termination or by doping with impurities. Increasing the conductive of diamond films is important if diamond films are going to be used as electrochemical electrodes and electronic devices. As of now boron is the most common p-type dopant for diamond and n-type films have been achieved with nitrogen doping of UNCD films.

3.1.1 Surface Conductivity of Hydrogen Terminated Diamond

In [73], Landstrass and Ravi described the substantial surface conductivity of hydrogen-terminated single crystalline diamond; they also reported similar results for as-grown MPCVD diamond films [73]. They found that hydrogen terminated diamond films were more conductive before annealing in atmospheric conditions (dehydrogenation) Several suggestions have been made to account for this phenomenon including the formation of shallow acceptor states which was first postulated by Landstrass and Ravi *et al.* in [73]; passivation of deep defects [74] and finally adsrobate based transfer-doping mechanism[75-79]. Recent results by authors such as Maier, Ristein and Williams [75-79] support the transfer-doping model, which requires not only the present of hydrogen, but the formation of anions in a thin aqueous layer above the hydrogen-terminated

surface. They propose a mechanism were electrons transfer from the valence band to absorbates at the surface which results in the formation of a dipole with a hole accumulation layer just beneath the surface. Electrons transferred from the surface to the aqueous layer via the following redox reaction $2H_3O^+ + 2e^- \Leftrightarrow 2H_2 + 2H_2O$. Figure 16 shows both the hydrogen terminated surface in contact with the aqueous layer as it appears in air and the band bending during electron transfer. Ristein verified this conclusion in [77] by heating samples in an ultra high vacuum which removes the aqueous layer while preserving hydrogen termination. The resulting diamond films became highly resistive again. The original conductivity of these films was restored when the films were re-exposed to the atmosphere. These result confirm that hydrogen termination along is not responsible for the increased conductivity see Table 4 for a lists of properties associated with hydrogen terminated diamond films.

Researchers have attempted to use hydrogen terminated diamond films for electronic applications. For example, Garrido [80] and his colleagues fabricated in-plane transistors using a combination of lithography and surface oxidation on hydrogen terminated polycrystalline diamond. These devices demonstrate low leakage current at 77 K and room temperature with good saturation and complete pinch-off. Aleksov $et\ al.$ [81] reported fabrication of RF FETs with a gate length of 0.2 um. This device produced a maximum output current of I_{Dmax}=360 mA/mm with a peak transconductance of 148 mS/mm, however current instabilities at microwave frequencies prevent this device from being used in high power applications.
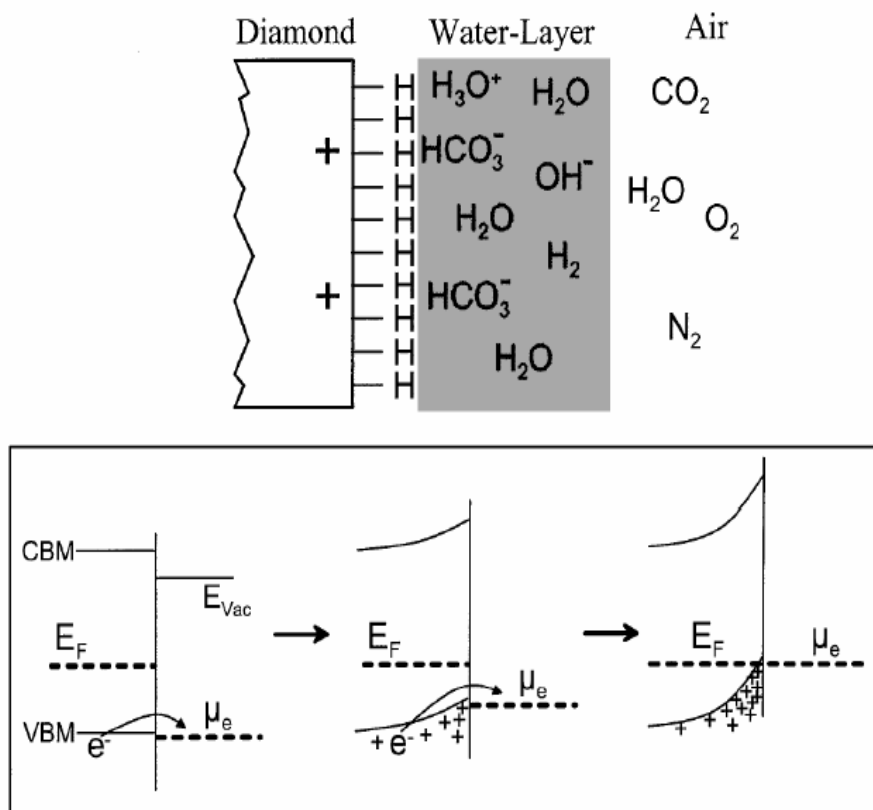
Figure 16. Top: Schematic representation of a hydrogen terminated diamond surface in contact with an aqueous layer as it forms in air. Bottom depicts the evolution of the band bending during the electron transfer process at the interface. [78]

Table 4.
Properties of Hydrogen Terminated Diamond [78]

Surface Conductivity	$\sim 10^{-4} - 10^{-5}$ ohm^{-1}cm^{-1} at room temperature RT
Density of p-type carries	$\rho_s = 10^{13}$ cm^{-1} hardly temperature dependent between RT and 150K $(\sim T^{1.5})$
Hall mobility of carriers	30 cm^2 V^{-1} s^{-1} Max value of 70 cm^2 V^{-1} s^{-1} temperature dependency $(\sim T^{1.2})$
Negative Electron Affinity	H-terminated diamond surfaces can be used as electron emitters

3.1.2 Boron Doping

Boron is a naturally occurring dopant or impurity found in natural diamonds. In fact, type IIb diamond demonstrates p-type conductivity with a boron concentration less then 1ppm. To date, boron incorporation has been accomplished via gas reactants, solid sources i.e. boron power, boron oxide [82] and cold implantation rapid annealing CIRA [83]. Other well known dopants are diborane [84, 75] and trimethayoboron $B(C_2H_5)_3$[86, 87].

Extensive research has been conducted on boron doped natural diamond films to determine their electronic properties. Okushi *et al* [86] achieved homoepitaxial doped boron diamond films with hall mobilities of 1840 cm^2 V $^{-1}s^{-1}$ at 290 K using $CH_4/H_2/B(CH_3)_3$. Hatta [84] reported hall mobilities of 1600 cm^2 V $^{-1}s^{-}$ with a hole concentration $> 10^{14}$. In addition Tsubota [87] produced homoepitaxial diamond with hall mobilites of 2020 $cm^2 V^{-1}s^{-1}$ at 243 k with a hole concentration of $5x10^{12}$ cm^{-3} it should be noted that this value was only obtained after exposure to hydrogen plasma. Table 5 shows the hall mobility and hole concentration for homoepitaxial grown diamond using boron doping.

As of now, boron doped diamond films have primarily been used as electrochemical electrodes. Electrodes have been constructed on poly [88], nano [89] and ultrananocrystalline diamond films [90]. These electrodes demonstrate low background currents, wide working potentials and are responsive to many solutions i.e. $Fe(CN)_6$ $^{3-/\,4}$ and $IrCl_6$ $^{2-/3-}$ and Fe $^{3+/2+}$ [90].

Table 5.
Comparison of Hall Mobilities and Hall Concentration for Boron Doped Diamond

Authors	Boron Source	B/C (ppm)	Hall Mobility $cm^2V^{-1}s^{-1}$	Substrate Temperature (K)	Hall Concentration (cm^{-3})
Homoepitaxial Growth					
Tsubota et al [87]	TMB	100	2020	243	$5x10^{12}$
Hatta et al [84]	B_2H_6	10	1600	290	$5.0x10^{13}$
Kiyota et al [23]	B_2H_6	20	1000	293	10^{14}

3.1.3 Nitrogen Doped Ultrananocrystalline Diamond

Highly conductive nitrogen doped n-type UNCD diamond films have been deposited using MPCVD [91]. The conductivity of nitrogen doped UNCD films increases five orders of magnitude with increasing nitrogen content as compared to un-doped films. Other electrical properties of nitrogen doped UNCD films such as carrier concentration, electron mobility and sheet resistivity have also been studied. Bhattacharyya *et al.* in [91] used Hall Effect measurements to determine the carrier density and moblilities of 10 and 20% nitrogen doped UNCD films. They reported high carrier concentration of 2.0×10^{19} and 1.5×10^{20} cm^{-3} for 10% and 20% doped films. Carrier mobilities of 5 and 10 cm^2/Vs were also measured for 10 and 20% films [91]. However, Williams *et al.* in [92] reported lower carrier mobilites of 1.48 and 1.56 cm^{2}V^{-1}s^{-1} for 10 and 20% films at room-temperature. Williams also calculated the sheet resistivity of nitrogen doped UNCD films. Room-temperature sheet resistivity increased from 22 ohm/sq for 20% N$_2$ film, to 880 ohm/sq for 10% N$_2$ films and finally 2.5 $\times 10^4$ ohm/ sq for 5% N$_2$ film [92].

Zapol [93] and others [91-94] propose that the high conductivity of these films is the result p-bonded carbon atoms in the grain boundaries. In their model, nitrogen is incorporated into grain boundaries giving raise to bands of mid-gap states. As a result, hopping conduction or other thermally activated conduction mechanisms could lead to enhancement of electronic conductivity. There is also evidence which suggests that nitrogen addition to the plasma leads to changes in the film structure of UNCD. For example Birrell *et al.* in [94] showed that nitrogen incorporation into UNCD films results in increased grain size, wider grain boundaries, and a slight increase in sp^2 bonded carbon. The gas chemistry and growth mechanisms of UNCD is also effected by nitrogen

addition; optical absorption spectra indicates there is a large amount of CN [48] present when nitrogen is introduced in various amounts as opposed to mainly C_2 dimmers in Ar/CH$_4$ spectra. The actual role of CN in the growth of nitrogen doped UNCD films is still being investigated. One point of view is that CN reduces renucleation rates [93] of UNCD much like hydrogen in CH$_4$/H$_2$ chemistries. This view would account for the increased grain size of nitrogen doped UNCD films with increasing N$_2$ content. However, more studies are needed to determine the role of CN in UNCD film growth.

Nitrogen doped films are now being considered for several applications including electrochemical electrodes as well as electronic devices [95]. Like boron doped electrochemical electrodes nitrogen doped electrodes exhibit a wide working potential window, low background current, and a high degree of electrochemical responsiveness for Fe(CN)$_6^{-3/-4}$, Ru(NH$_3$)$_6^{+3/+2}$ and IrCl$_6^{-2/-3}$ [96]. However, these electrodes are not as good as boron doped electrodes because their electrical responses are dependent on physicochemical properties of the grain boundaries [90].

CHAPTER 4

EXPERIMENTAL PROCEDURES

4.1 System description

The experimental set-up for the microwave CVD reactor is shown in Figure 17. The chamber consists of a quartz bell jar, which is enclosed in a Faraday cage. Microwave power is supplied by a water-cooled ASTEX 2.45 GHz waveguide. The chamber itself is connected to a mechanical vacuum pump and the chamber pressure is controlled by a throttle valve. Reactant gases are introduced into the chamber by a small inlet on the side of the reactor. Gas flow rates of N_2, CH_4, and Ar are controlled by mass flow controllers. Samples are load onto a cylindrical stainless steel holder and Mo plates are used to adjust the distance between the substrate and the plasma. The substrate temperature is measured using an optical pyrometer. The chamber also has two inlets where air is circulated to provide cooling for the bell jar. The whole system is monitored by two safety interlocks; the first monitors the ultraviolet light generated by the plasma and cuts the power off if the plasma ball disappears. The second interlock measure the water flow for cooling the microwave generator.

4.2 Substrate Preparation

Nitrogen doped diamond films were grown on Si, SiO_2 and quartz. Films grown on SiO_2 substrates were used for conductivity measurements. Substrates were cleaned ultrasonically in acetone and methanol for ten minutes followed by a two step nucleation
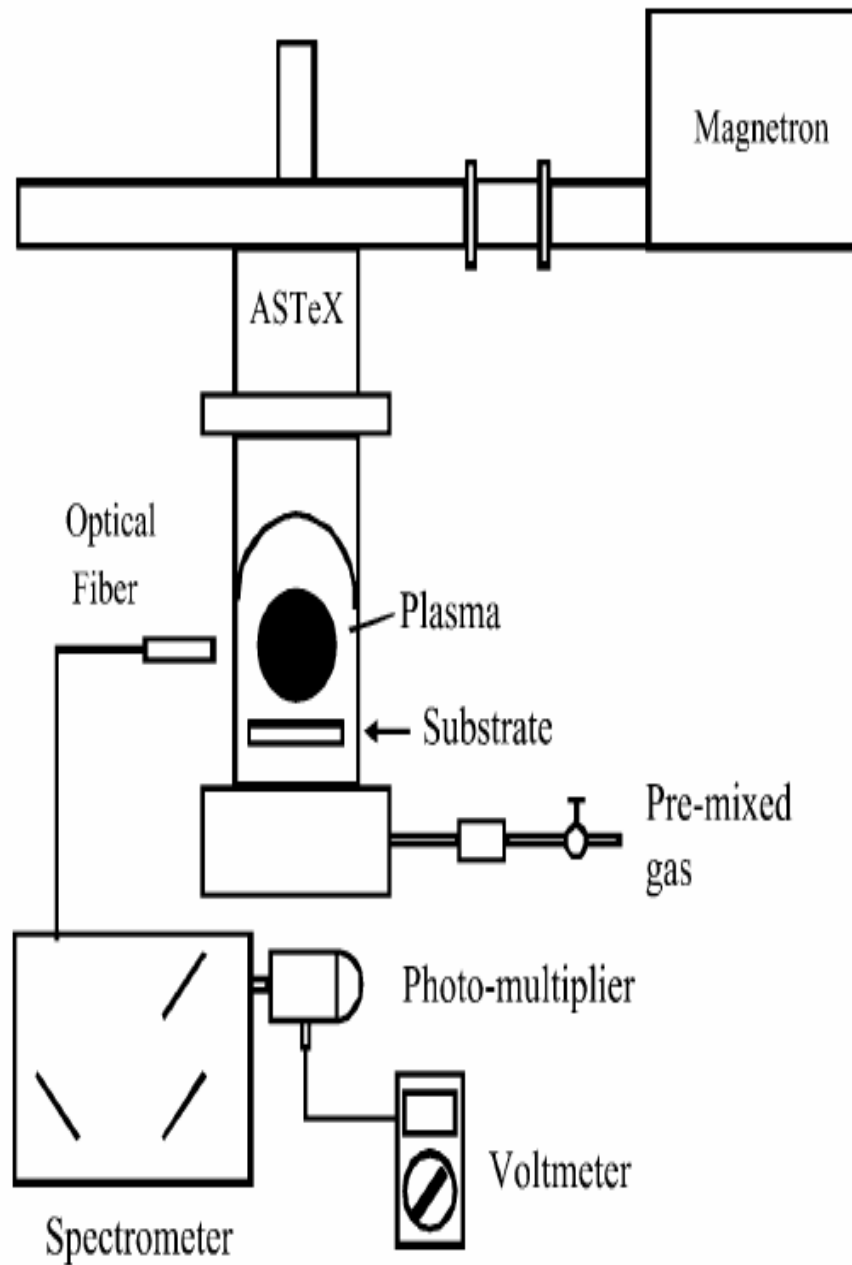
Figure 17. ASTeX 5010 reactor [95]

process. First samples were nucleated with an amorphous carbon layer via (97%Ar/2%H_2/1%CH_4) plasma for 10 mins. Next, the substrates were ultrasonically agitated in nanodiamond and methanol solution for 30-60 mins. Samples where then washed with methanol and isopropyl alcohol before growth.

4.3 Experimental Procedures

Prior to deposition the chamber pressure was pumped down, then gas reactants were introduced to the chamber. The microwave power varied between 600 and 800 Watts while the chamber pressure was held constant at 100 Torr. The substrate temperature was estimated to be 786°C - 894°C by an optical pyrometer it should be noted that the actual substrate temperature was not determined. NCD films were deposited using CH_4/N_2/Ar plasma. The total flow rate was kept constant at 100 sccm during all experiments, as the nitrogen content was varied between 0-40 sccm the Ar flow rate was adjusted. Films were then characterized by SEM, Raman, four point measurements and electron emission current measurements.

4.4 Diamond Film Characterization

Raman scattering is an important nondestructive tool for identifying diamond films. For this experiment visible Raman spectra were obtained on all samples using a He-Cd laser with a 100mW excitation photon (441.6 nm). The focus size of the laser beam is 8mm.

Scanning electron microscopy (SEM) is another tool used to characterize diamond films. SEM images can be used to establish the morphology of the diamond films. It can also be used to determine the relative thickness of the diamond films as well as the growth rate.

CHAPTER 5

RESULTS

5.1 Field Emission Properties

Nitrogen doped NCD films were deposited on (100) n-type silicon substrates for emission analysis. Electron emission tests were conducted in an evacuated chamber with a diode structure. The ambient pressure in the test chamber is $\sim 10^{-6}$ Torr; the actual test setup is depicted in Figure 18. This setup consists of a top electrode made from a metal rod encased in a ceramic block; a pica-ammeter, which is used to measure the emission current, and a high voltage source. Two 60 um Al_2O_3 spacers were used to separate the substrate from the electrode. It should also be noted that the edges of all samples were cut prior to the emission test to ensure there was no connection between the diamond film and the silicon substrate on the side of the sample.

For this measurement we define the turn on electric field as the electric field at which the emission current is equal to $1.0x10^{-7}$ Amps. The Log (I) - E characteristic for NCD films grown at 600 and 800 Watts are plotted in Figure 19. The emission properties of these films increase with increasing nitrogen in the plasma. In films grown at 600 watts the turn on electric fields decreases from > 50V/um to 40 V/um with 10 and 20% nitrogen respectively. Similar results have been established for 800 Watts samples with turn on electric fields of 50 V/um and 35 V/um with 10 and 20% nitrogen addition.
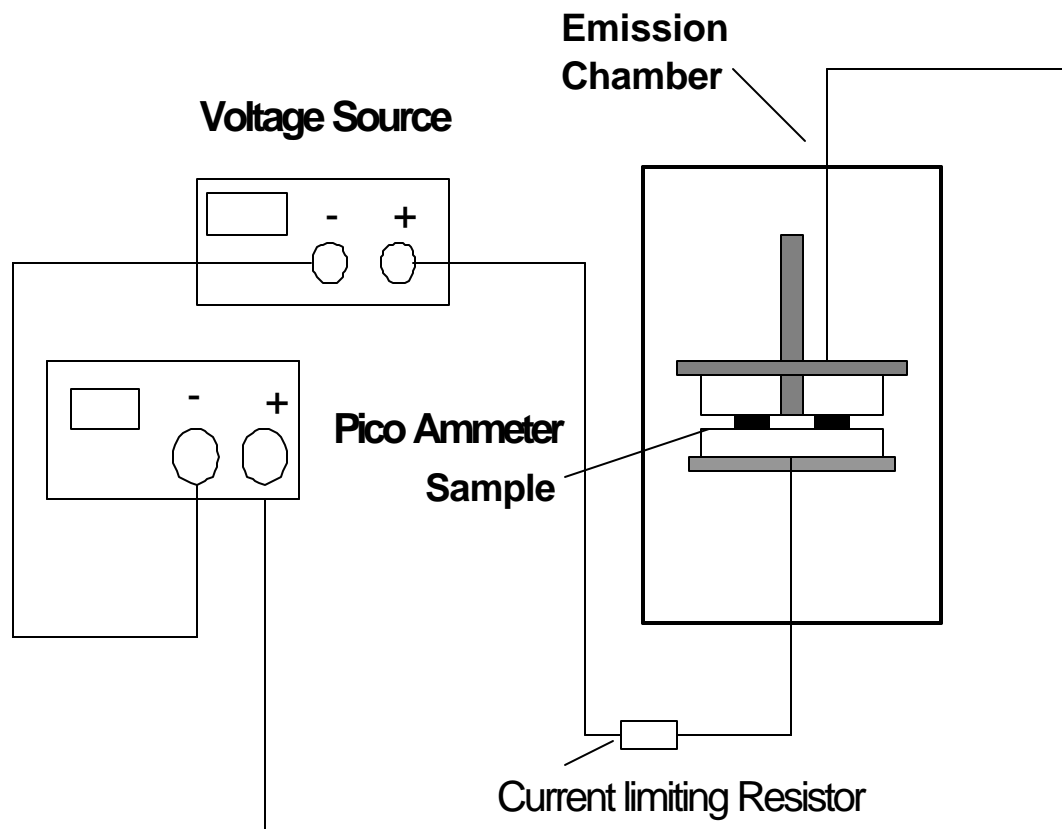
Figure 18. Setup for Emission Current Measurements

a)

b)
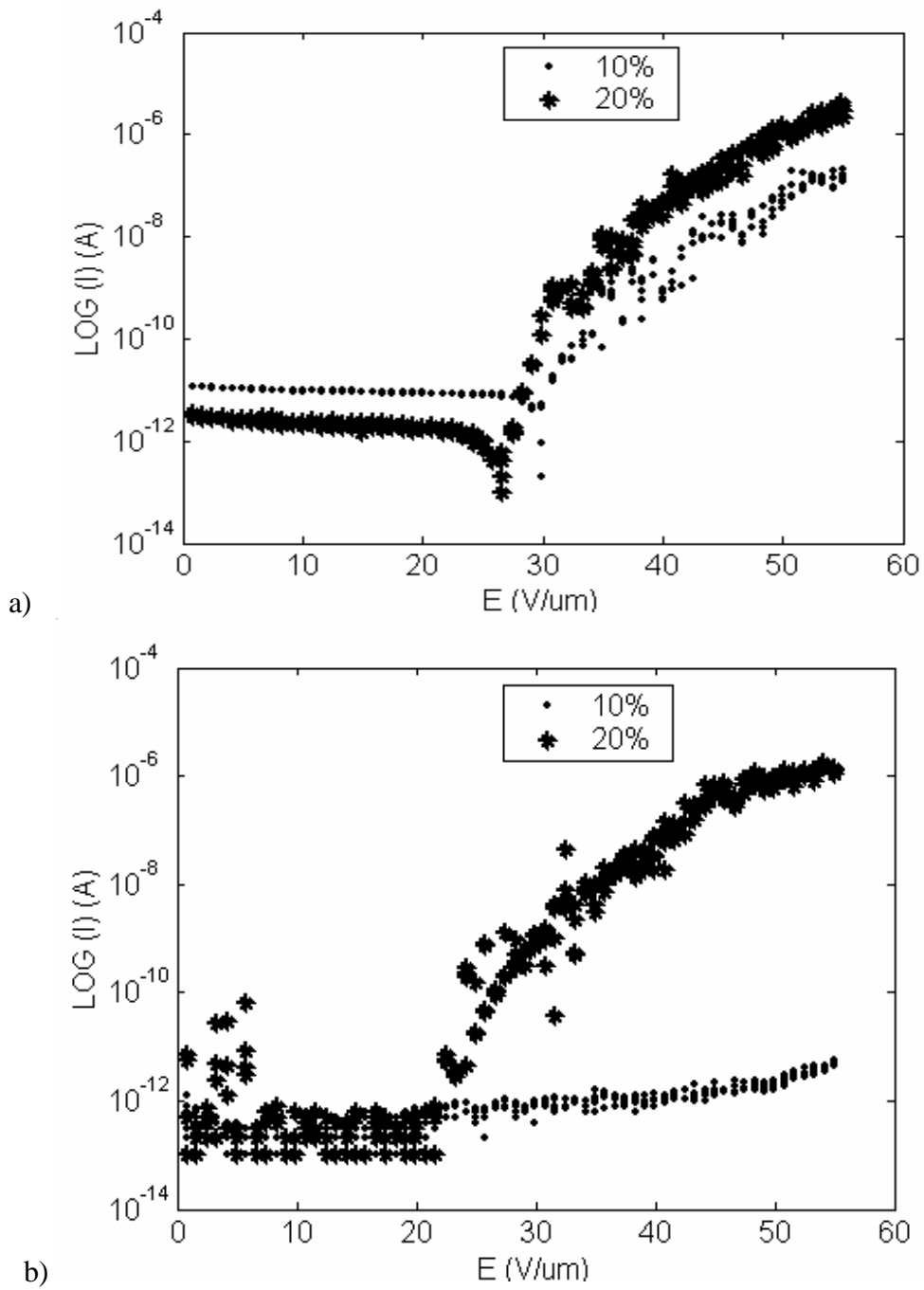
Figure 19. Log (I)-E curves for 800 and 600 Watt nitrogen doped NCD films. Increased nitrogen content results in decreased threshold voltages from a) >50 to 35 V/um b) > 50 to 40 V/um respectively

Figure 20 displays the I-V characteristic for 600 and 800 watt NCD samples. When the N_2 flow is increased from 10 to 20%, the emission current at 30 V/um increases 2 orders of magnitude from 10^{-11} to 10^{-9} Amps for 800 Watt films. Comparable results are seen in 600 Watt films where the emission current is 3 orders of magnitude higher for 20% samples. It should be noted that 5% and 40% samples did not admit even at very high electric fields. Additionally, the linear nature of the Fowler-Nordheim (F-N) plots in Figure 21 shows that the emission characteristic of these films is the result of electron tunneling.
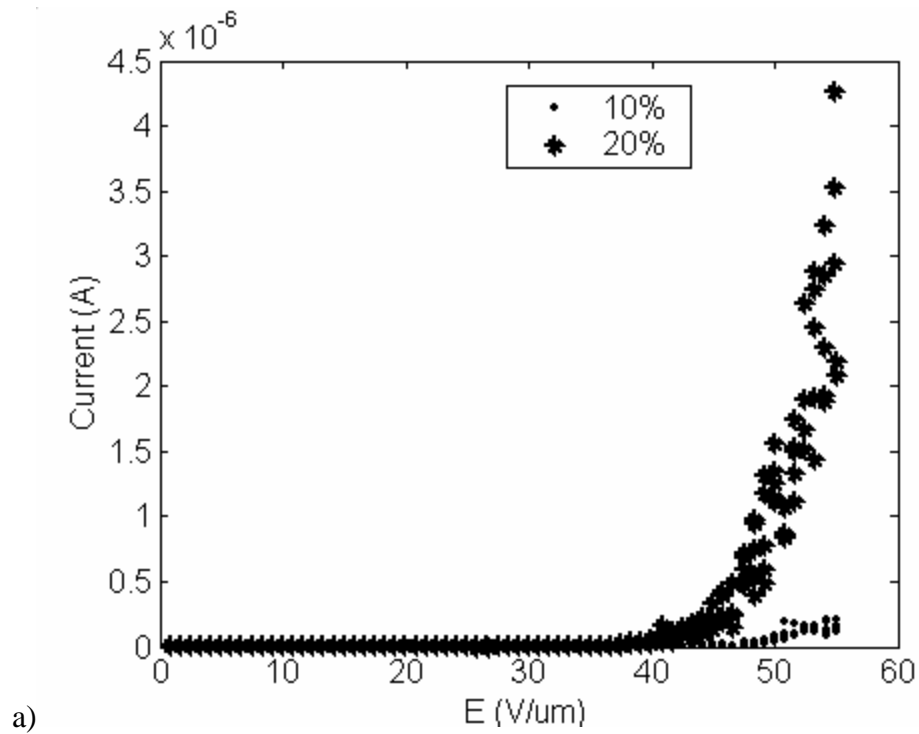
a)
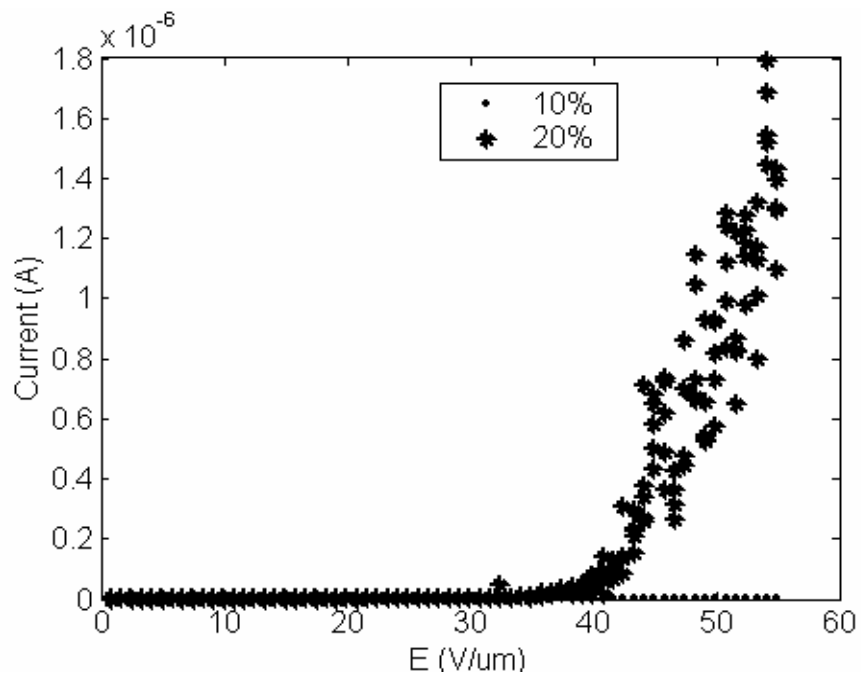
b)

Figure 20. I-E curve for 800 and 600 Watt nitrogen doped NCD films. Increased, nitrogen content in the plasma results in increased emission current for a) 800 and b) 600 Watt films
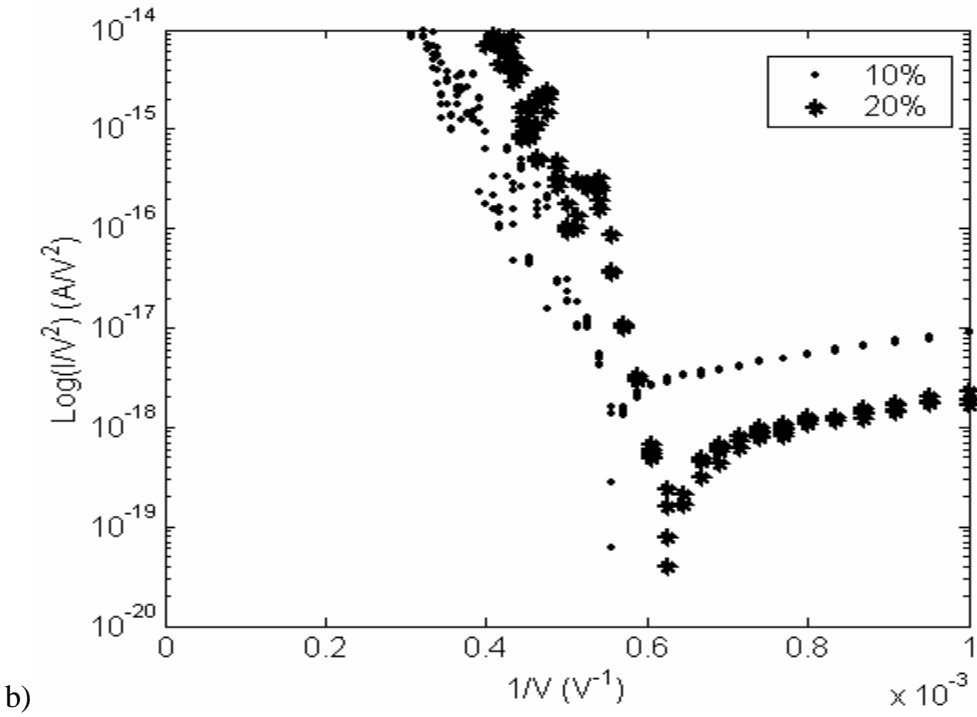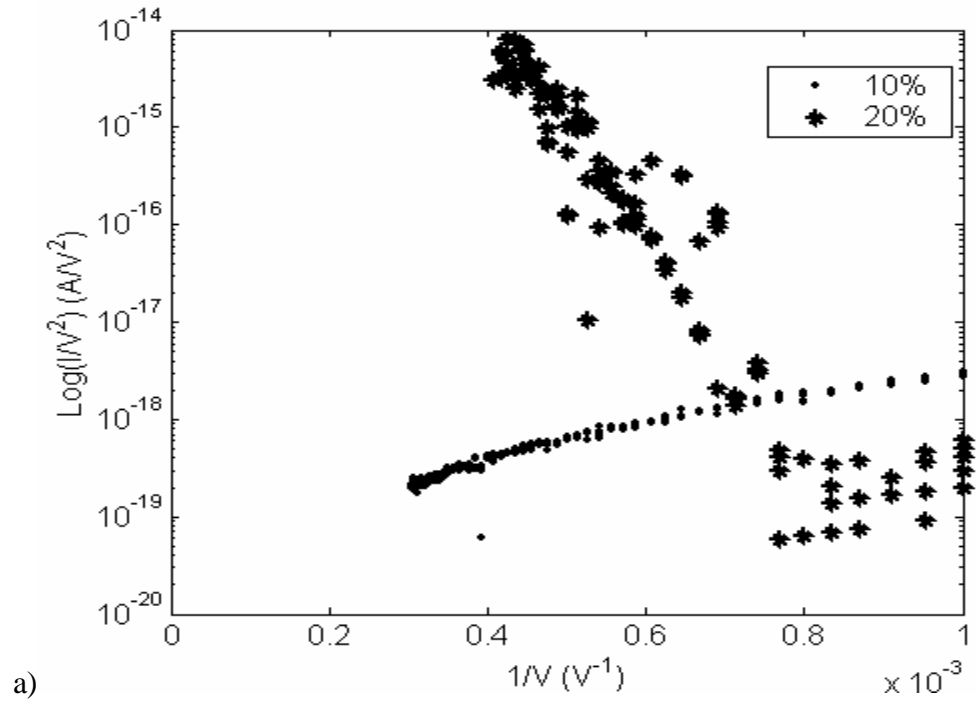
Figure 21. F-N plots for 10 and 20% nitrogen samples grown at a) 600 and b) 800 Watts.

5.2 Surface Roughness as Function of Nitrogen Concentration

The surface roughness of doped NCD films was evaluated using an Alpha-step 200 surface profiler. A scan length of 80 um with a scan rate of 25 scans per um was used during testing. The surface roughness of doped NCD films gradually decreases with nitrogen content for both 600 and 800 Watt samples. With 10% nitrogen added to the plasma the roughness of 600 and 800 Watts films is approximately 20 to 24 nm. The addition of 20% nitrogen to the plasma leads to roughness values between 12-15 nm for 600 and 800 Watt films. The 800 Watt film grown with 40% nitrogen had a roughness of ~8 nm. These results are consistent with those of Peng et al [98]. The reduction in surface roughness is believed to be the result of CN which increases in the plasma with increasing nitrogen content.

Figure 22 shows the optical emission spectrum for $Ar/N_2/CH_4$ plasma which shows that C_2 is the dominant species in the plasma when nitrogen is not present, but as nitrogen is introduced three other emission signals appear at 678.7nm (N_2), 421.6 and 460.6nm (CN). It is the CN emission which becomes larger with the addition of nitrogen that is thought to be important in this process. Further study needs to be conducted to determine the role CN plays in $CH_4/Ar/N_2$ microwave plasma.
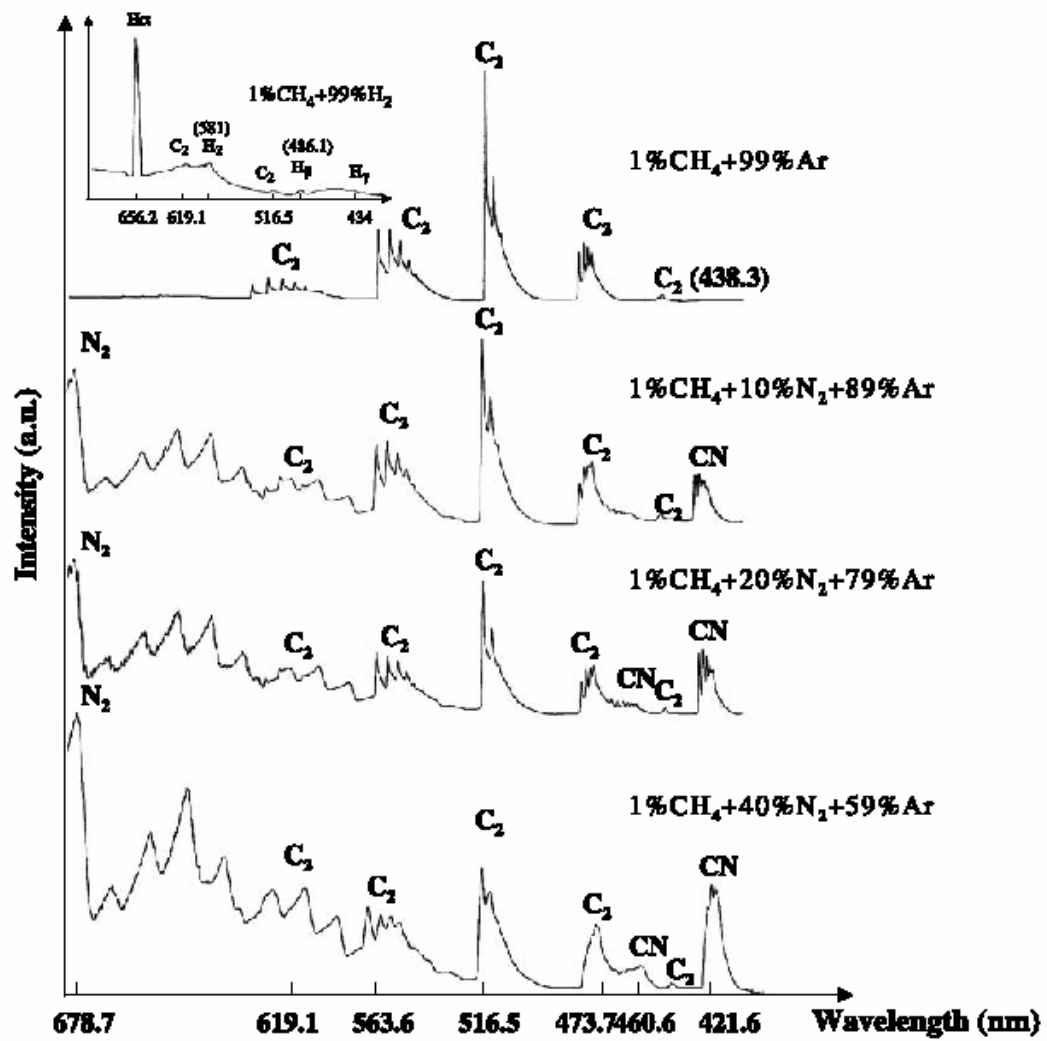
Figure 22. Optical emission spectrum for nitrogen doped NCD films with 10, 20, and 40% nitrogen addition [95]

5.3 Characterization of Nitrogen Doped NCD films

NCD films have been characterized using raman spectrum as well as scanning electron microscopy (SEM). The raman spectra for nitrogen doped diamond films are shown in the Figure 23 and 24. There are three main peaks which occur at 1160, 1350, and 1550 cm^{-1}. The first peak at 1160 cm^{-1} is typically used to indicate NCD phases in the diamond films. However, researchers like Ferrari *et al.* [99] have shown that this peak is related to sp^2 sites and assign its origin to polyacetylene lying in the grain boundary. The other two peaks at 1350 and 1550 cm^{-1} represent the D and G bands. The addition of nitrogen during growth causes the 1332 cm^{-1} peak to broaden and the peak at 1350 cm^{-1} becomes more dominate. Additionally as nitrogen is increased in the plasma the raman intensity decreases and all three of the peaks broaden.

Cross-sectional SEM images of several NCD films are shown in Figures 25 and 26. When N_2 is increased from 10 to 20% the growth rate for 600 Watts samples increases from 0.8 to 1.14 um/hr. 800 Watt samples show almost identical results with growth rates of 0.7 and 1.07 um/hr with 10 and 20 N_2 addition respectively. Figures 27 and 28 shows SEM images of both 600 and 800 Watt films. These images along with Raman confirm that the diamond films deposited here are in fact nanocrystalline in nature.
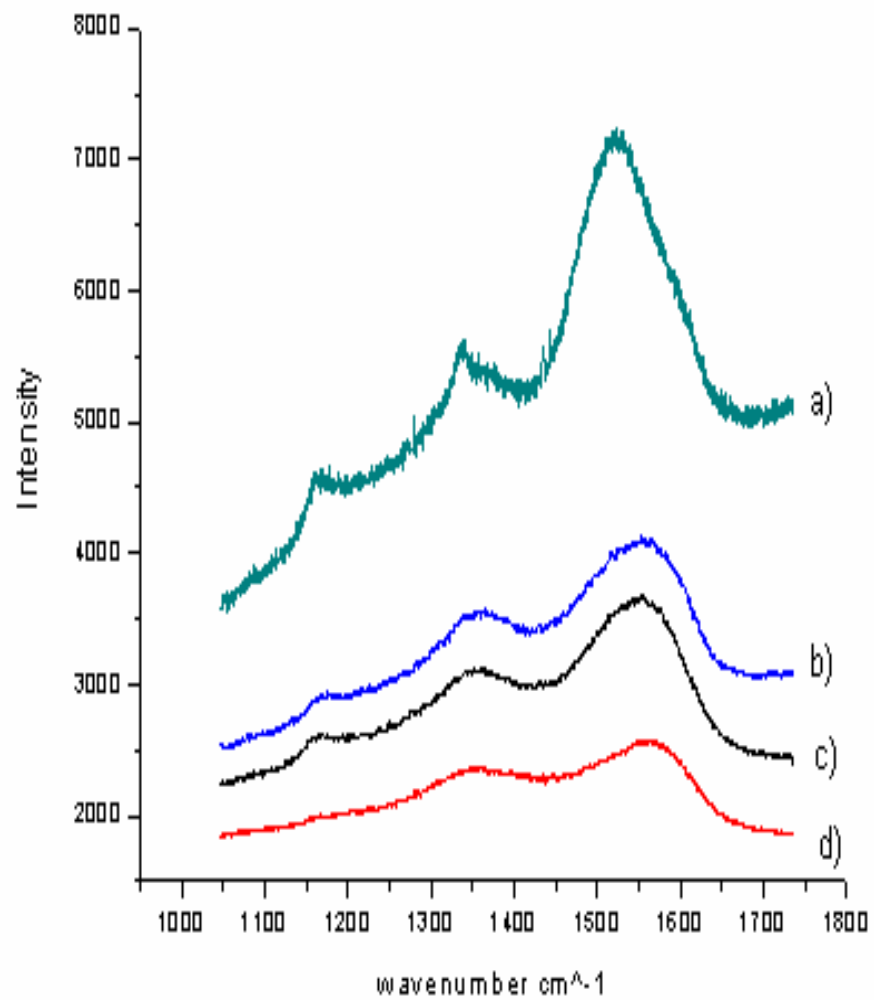
Figure 23. Raman spectra of NCD films grown with $CH_4/N_2/Ar$ plasma at 600 Watts with varying nitrogen content a) 0 b) 3 c) 10 and d) 20%.
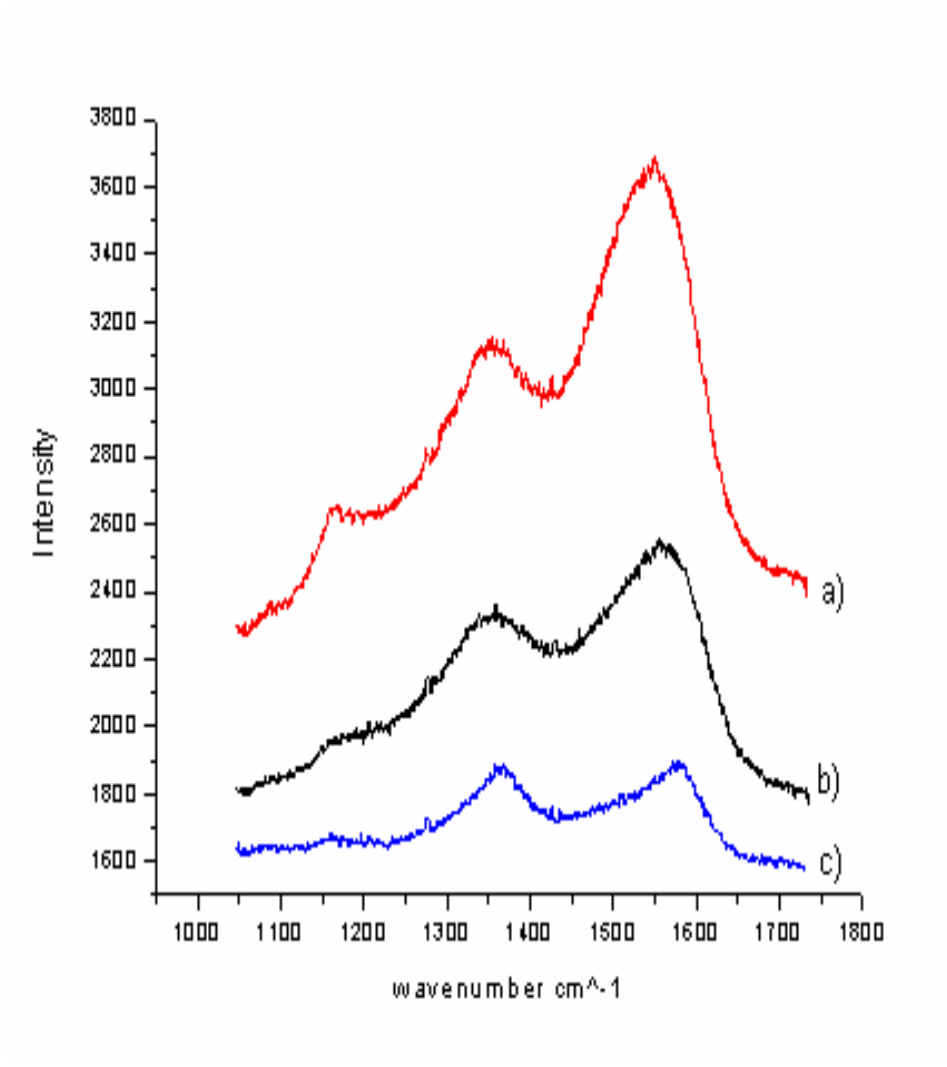
Figure 24. Raman spectra of NCD grown at 800 Watts with a) 10 b) 20 and c) 40%
nitrogen .
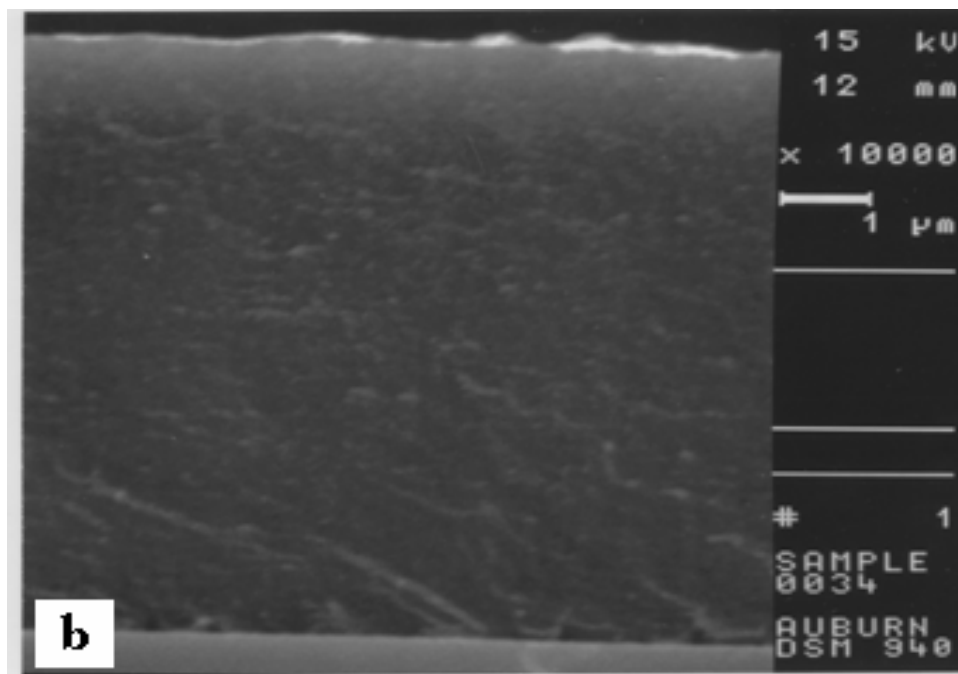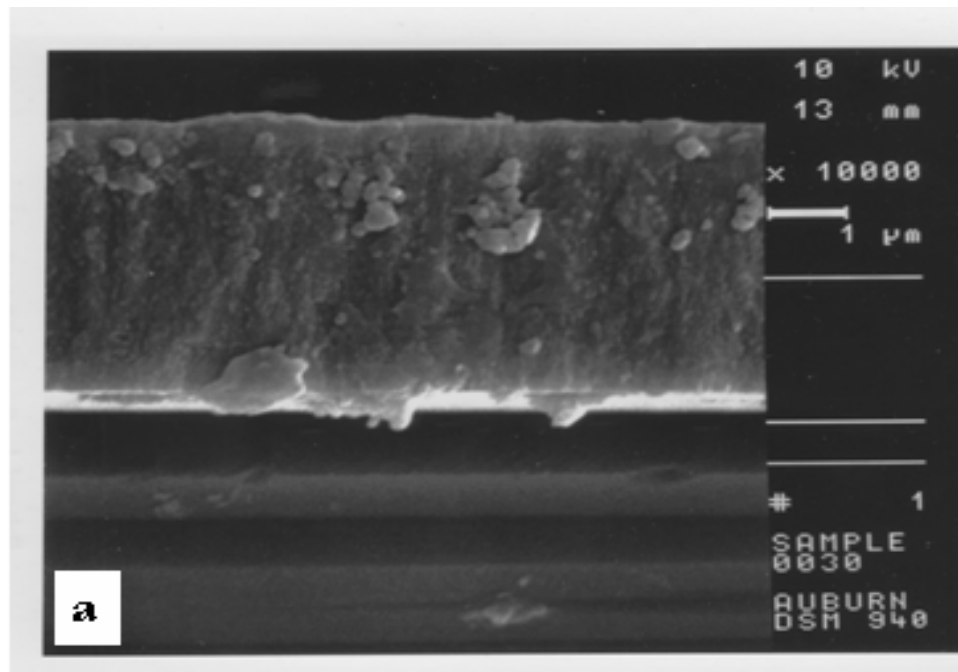
Figure 25. SEM of 600 Watt NCD films grown with a) 10 and b) 20 percent nitrogen.
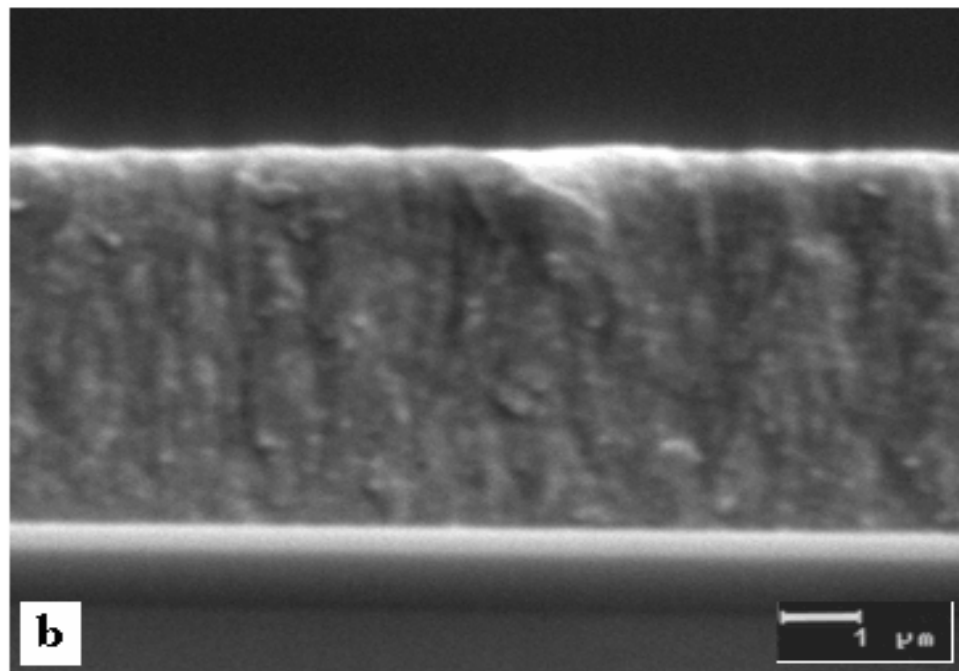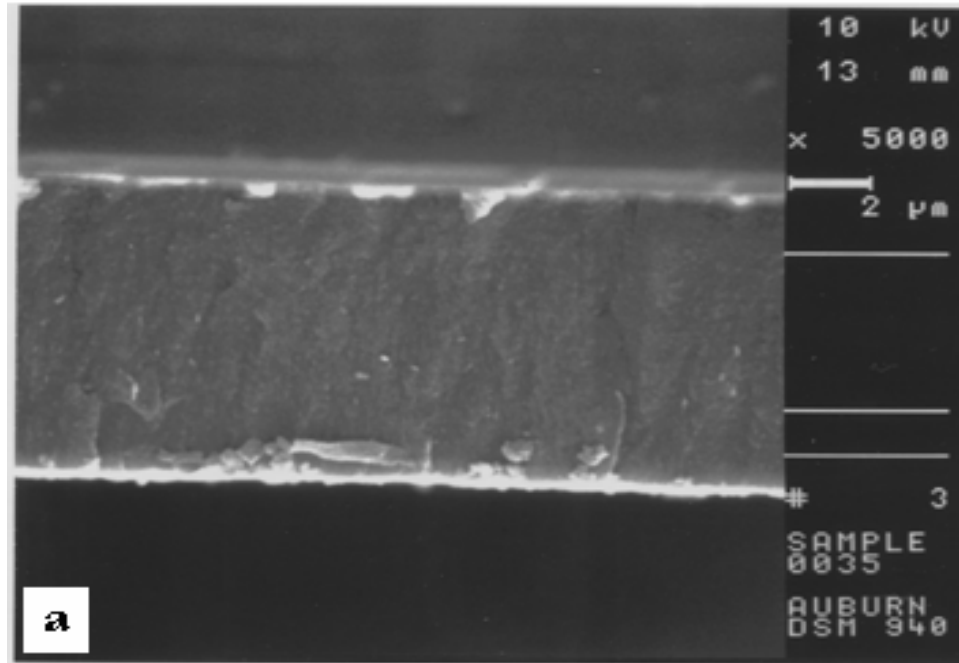
Figure 26. Cross-sectional SEM images of 800 Watt films grown with a) 10 and b) 20 % N_2
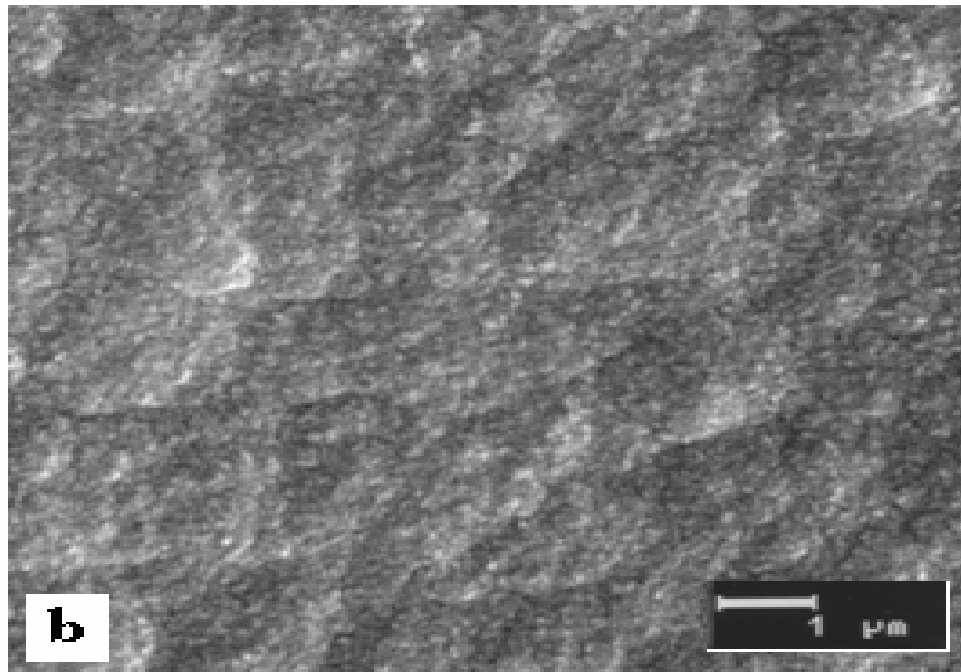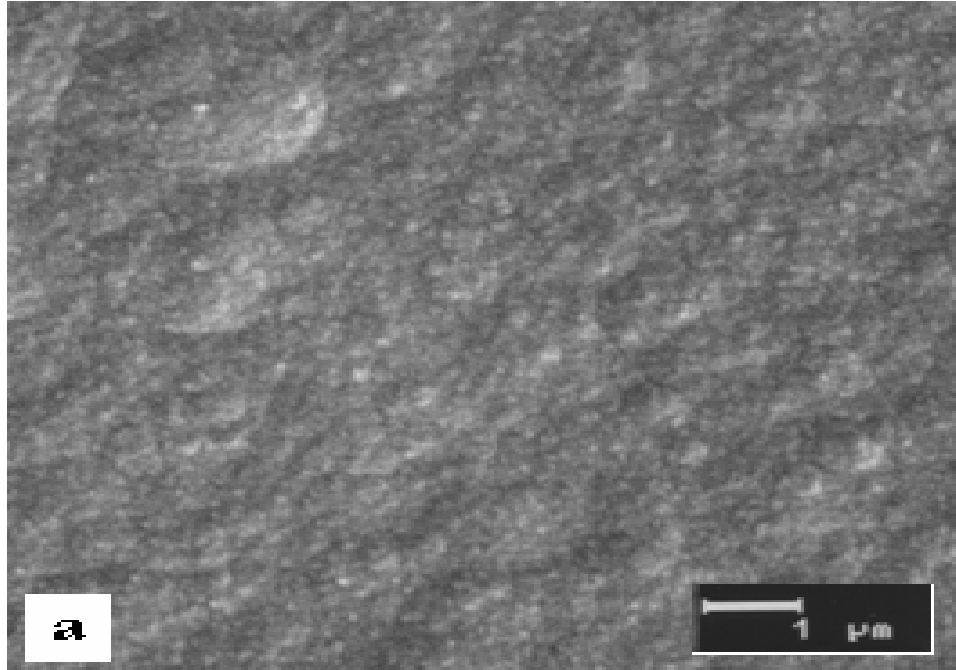
Figure 27. SEM image for 600 Watt NCD films grown with a) 10% and b) 20% nitrogen.
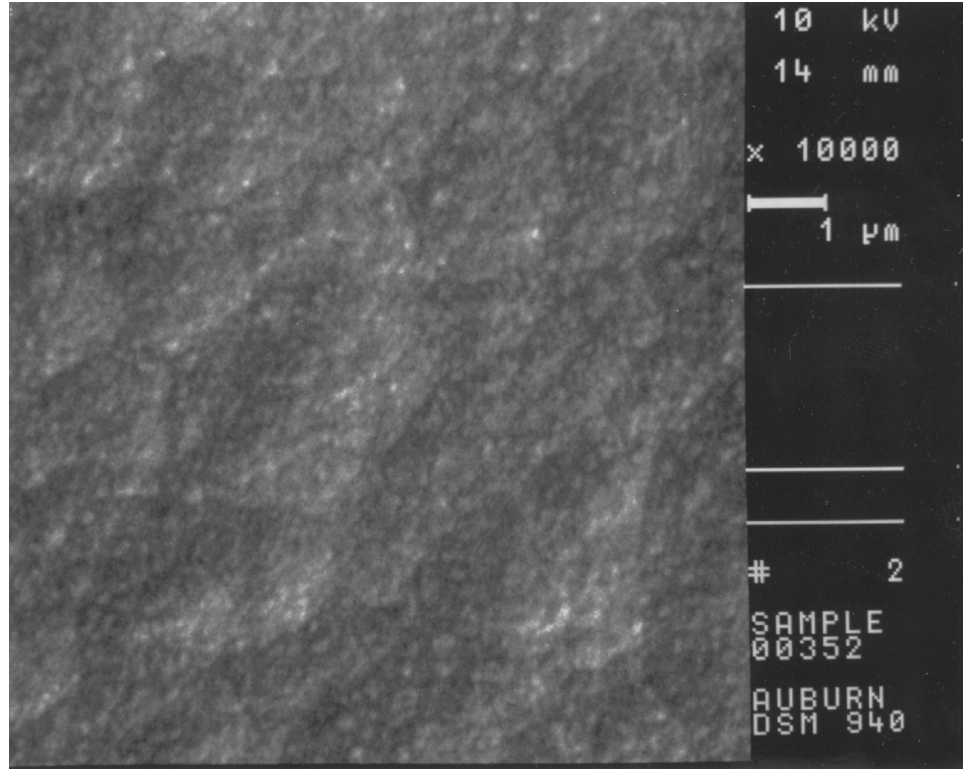
Figure 28. SEM image of nitrogen doped 800 Watt film with 20% nitrogen.

5.4 Conductivity of Nitrogen Doped Diamond Films

The conductivity of nitrogen doped NCD films was measured using and a four point probe configuration. Figure 29 shows the four point contact structure. All measurements were done using an HP 4145 analyzer. In this particular setup, current is forced across the outer contacts, while the voltage is measured across the two middle contacts. Resistivity values were calculated using the following equation:

$$\text{Resistivity} = t\left(W/L\right)\left(V/I\right) \ \text{ohm-cm}$$

where t is equal to the thickness of diamond film, L is the distance between the two middle contacts, W is the width of the diamond films and I and V represent the applied current and the measured voltage respectively.

The resulting diamond films demonstrate increased conductivity with increasing nitrogen addition during growth. The conductivity of 800 Watts samples is 0.191 ohm^{-1}cm^{-1} for 20% samples while 10% samples show lower conductivity around 4.0×10^{-4} ohm^{-1}cm^{-1}. On the other hand 600 Watts samples grown with 10 and 20% nitrogen additions have conductivity values of 1.05 and 5.55 ohm^{-1}cm^{-1} respectively. The 600 watt samples demonstrate a higher conductivity than do the 800 watt samples.

These results show conductivity NCD films can be grown by adding nitrogen to CH_4/Ar plasmas. These results are not as high as those reported by Argonne National Labs. This can be expected because we used a different reactor which has a higher power density; additionally the substrate temperature is not maintained at 800°C during growth. These are just a couple of factor which may affect the conductivity of nitrogen doped methane/argon plasmas. Therefore more work is needed to determine the role of substrate heating during deposition of CH_4/Ar/N_2 plasma.
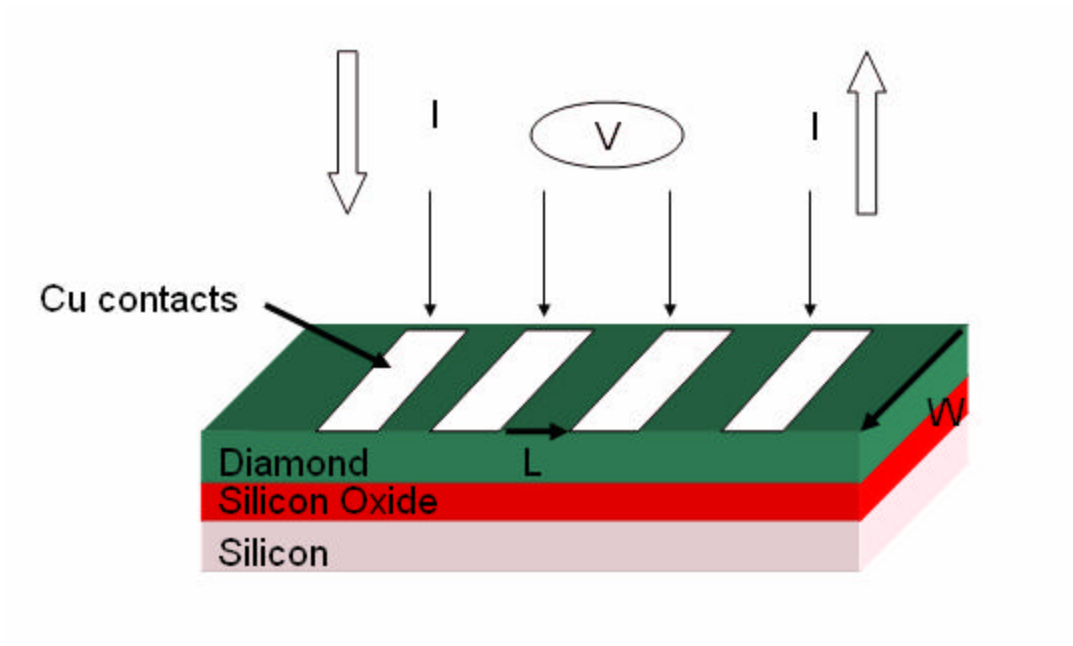
Figure 29. Four point contact configuration

CONCLUSION

Nitrogen doped diamond films have been successfully deposited onto several substrates including silicon, silicon dioxide, and quartz. These films have been studied to determine their electrical, emission and surface properties. The resulting data indicates that nitrogen addition results in increased conductivity as well as increased emission current and lower turn on electric fields. The surface roughness of the samples decreased with increased nitrogen content which believe to be a consequence of (CN) in the plasma. The nitrogen doped films grown here are more like those grown using CH_4/N_2 [28] reactant gases, where the emission properties are controlled by the ratio of methane to nitrogen. The raman spectra of these films are identical to those reported here; also the emission behavior and growth rates are similar to ours. Therefore it is believed that the conditions reported here are in a regime between low emitting CH_4/N_2 films and conductive $CH_4/Ar/N_2$ films. Additionally the results show how important it is to maintain the substrate at constant temperature during growth. Further studies are needed to determine the relationship between substrate temperature and nitrogen concentration in films.

BIBLIOGRAPHY

1.   Kohn, M. Adamschik, P. Schmid S. Ertl, A Floter, *"DIAMOND MEMS-FROM PROOF -OF- CONCEPT TO APPLICATION"*, Proc. ADC/FCT 1999, pp 420-424, August 31- September 4, 1999, Tsukuba, Japan

2.   A. Hartl, E. Schmich, J.A. Garrido, J. Hernando, Slivia C. R. Catharino, S. Walter, P. Feulner, A. Kromka, D. Steinmuller and M. Stutzmann, *Nature Materials* vol 3 iss. 10, (2004) 682-686

3.   S. Ida, T. Tsubota, S. Tanii, M. Nagata, and Y. Matsumot., Langmuir 2003, 19, 9693-9698

4.   M. Ishihara, T. Nakmura, Y. Koga and F. Kokai, *"CHARACTERIZATION OF AIN AND $LiNbO_3$ THIN FILMS DEPOSITION ON DIAMOND SUBSTRATES"*, Proc. ADC/FCT 1999, pp 420-424, August 31- September 4, 1999, Tsukuba, Japan

5.   H. Nakahata, S. Fujii, K Higaki, A Hachigo, H. Kitabayshi, S. Shikata and N. Fujimori, *Semicond. Sci. Technol.* 18 (2003) S96- S104

6.   A. Lettington, J. W. Steeds, *"Thin Film Diamond"*, Chapman & Hall, New York 1994

7.   K. E. Spears, Dismukes J.P., *"Synthetic diamond: Emerging CVD Science and technology"* , John Wiley & Son, INC NY 1993

8.   J. G. Angus, H. A. Will, and W. S. Stanko, (1968), *J. Appl. Phys.* 39, 2915-2922

9.   J. C. Angus, (1966), *Air Force Cambridge Research Lab Report*, AFCRL-66-107; AD-63-705

10.   F. P. Bundy , H. T. Hall, H. M. Strong, and R. H. Wentorf , (1955) *Nature* 176 51

11.   H. Liander, E. Lundblad, 1960 *Some Observation on the Synthesis of Diamonds*. Ark. Kemi. 16 139-149

12.   E. C. Vickery, (1973) *U. S. Patent* 3,714,334 30 January 1973

13. B. V. Deryagin, D. V. Fodoseev D. V, B. V. Spitsyn , L. L. Builov , A. A. Klochkov , A. E. Gurodetski, & A. V. Smolyaninove , 1976 *Synthesis of diamond on non-diamond substrates* Dokl. Akad. Nauk SSSR 231 333-335

14. S. Matsumoto, Y. Sato, M. Tsutsumi, N. Setaka, *J. Mater. Sci* 17 3106 1982

15. M. Kamo, Y. Sato, S. Matsumoto, and N. Setaka, *J Cryst. Growth* 62 642

16. M. S. Dresselhaus, G. Dresselhaus, P. C. Eklund, *Science of Fullerenes and Carbon Nanotubes.* Academic Press, Inc., San Diego, Ca (1996).

17. M. F. Ravet, A. Gicquel, E. Anger, Z. Z. Wang, Y. Chen, and F. Rousseaux, *"X-Ray Lithography Masks Based on Diamond Membranes: Potentiality and Realization"*, 2nd International Conference on the Application of Diamond Films and Related Materials pg 77 (1993)

18. Y. Tzeng , *"Microwave Plasma Enhanced Chemical Vapor Deposition of Diamond in the Vapor of Methanol-Based Liquids Solutions,* Proc of ADC/FCT 1999, pp 20-24, August 31- September 4, 1999, Tsukuba, Japan

19. Y. Tzeng , *"Hot-Filament Assisted Deposition of Diamond in the Vapor of Methanol-Based Liquid Solutions"*, Proc. ADC/FCT 1999, pp 420-424, August 31- September 4, 1999, Tsukuba, Japan

20. Y. Satito, K. Sato, K. Gomi, and H. Miyadera, *J. Mater. Sci.* 25 1246 (1993)

21. C. A. Rego, R. S. Tsang, M.N.R. Ashford, K.N. Rosser, *J. Appl. Phys*. 79 (9) (1996)

22. B. J. Bai, C. J. Chu, D. E. Patterson, R. H. Hague and J. L. Margrave, *J. Mater. Res*. 8 233 (1993)

23. J.-J. Wu, C.-H. Ku, T.-C. Wong, C.-T. Wu, K.-H. Chen, L.-C. Chen, *Thin Solid Films* 473 (2005) 24-30

24. P. W. May, *"Diamond thin films: a 21st - century material"*, Phil. Trans. R. Soc. Lond. A (2000) 358 473-495

25. D. Zhou, T. G. McCauley, L. C. Qin, A. R. Krauss and D. M. Gruen, *J. Appl. Phys*. 83 (1) 1998

26. D. M. Gruen , L. Shengzhong, A. R. Krauss, J. Luo, and X. Pan, *Appl. Phys. Lett*. 64 (1994) 1502

27.   D. M. Gruen, L. Shengzhong, A. R. Krauss, J. Luo, and X. Pan., *J.Appl. Phys*. 75, (1994) 1758

28.   K. Wu, E.G. Wang, and Z. X. Cao, *J. Appl. Phys*. 88 2967

29.   N. S. Xu, J. Chen, S. Z. Deng, K. H. Wu, and E. G. Wang, *J. Phys. D: Appl. Phys*. 33 (200) 1572-1575

30.   K. Kurihara, K. Sasaki, and M. Kawarada, and N. Koshino, *Appl. Phys. Lett*. 52 437 (1988)

31.   S. T. Lee, Z. Lin, X. Jiang, Material Science and Engineering, 25 (1999) 123-154

32.   Y. Hirose and M. Mitsuizumi, Jpn. *New Diamond Forum*, pg 27 (1990)

33.   C. Bednarski, Z. Dia, A-P., Li, b. Golding, *Diam. Relat Mater*. 12 (2003) 241-245

34.   M. Yoshikawa, H. Ishida, A. Ishitani, S. Koizumi, T. Inuzuka, *Applied Physics Letters*, Vol. 58 Issue 13 p1387 (AN 4330544)

35.   C. Yan, T.K. Vohra, H. Mao, R.J. Hemley, *PNS* vol 99 no 20 12523-12525

36.   C. Wild, R. Kohl, N. Herres, W, Muller-Sebert, and P. Koidl, *Diam. Relat. Mater*. 3 373 1994

37.   X. Ying, X. Xu, *Thin Solid Films* 368 (200) 297-299

38.   X. Ying, J. Luo, P. Wang, M. Cui, Y. Zhao, G. Li, P. Zhu, *Diam Relat. Mater*. 12 (2003) 719-722

39.   E. Woerner, C. Wild, W. Mueller-Sebert, P. Koidi, *Diam. Relat. Mater*. 10 (2001) 557-560

40.   J. E. Butler, The Electrochemical Society Interface, Spr. 2003 pg 22-26

41.   T. Lin, G. Y. Yu, A.T. S. Wee, and Z. X. Shen, *Appl. Phys. Lett*. 77 2692

42.   A.N. Jones, W. Ahmed, I. U. Hassan, C. A. Rego, H. Sein, M. Amar and M. J. Jackson, *J. Phys.: Condens. Matter* 15 (2003)

43.   T. Sharda, T. Soga, T. Jimbo, M. Umeno, *Diam. Relat. Mater*. 9 (2000) 1331

44.   C. Z. Gu and X. Jiang, *J. Appl. Phys*. 88 1788 (2000)

45. F. J. Guillen Hernandez, K. Janischowsky, W. Ebert, and E. Kohn., *Phys. Stat. Sol.* (a) NO. 11,2553-2557 (2004)

46. K. Subramanian, W. P. Kang, J. L. Davidson, and W. H. Hofmeister, *J. Vac. Sci. Technol. B.* 23 (2) 2005 pg 786

47. W. Yang, O. Auciello, J. E. Butler, W. Cai, J. A. Carlisle, J. E. Gerbi, D. M. Gruen, T. Knickerbocker, T. L. Lasseter , J. N. Russell Jr. L. M. Smith., R. J. Hamers, *Mat. Res. Soc. Symp. Proc.* Vol. 737 (2003) F4.4.1

48. O. Auciello, J. Birrell, J. A. Carlisle, X. X. Gerbi, B. Peng and H., D. Espiniosa *J. Phys.: Condens. Matter* 16 (2002) R539-R552

49. H. D. Espiniosa , B. Peng , K. H. Kim, B. C. Prorok, N. Moldovan,X. C. Xiao, J. E. Gerbi, J. Birrell, O. Auciello, J. A. Carlisle, D. M. Gruen, and D. C. Mancini., *Nano-and Microelectromechanical Systems (NEMS and MEMS) and Molecular Machines*, MRS Proc. vol. 741 J.9.2 (2002)

50. D. A. Horner, L. A. Curtissv, D. M. Gruen, *Chem. Phys. Lett*. vol 233 iss 243 (1995)

51. P. C. Redfern, D. A. Horner, L. A. Curtiss, D. M. Gruen *J. Phys., Chem*. vol 100 pg 11654, (1996)

52. M. Sternberg, M. Kaukonen, R. M. Nieminen, Th. Frauenheim , *J. Phys. Rev B* vol 63 pg 165414

53. M. Sternberg, P. Zapol, and L. A. Curtiss, *J. Phys. Rev. B* 68 205330 (2003)

54. X. Xiao, J. Birrell, J. E. Gerbi, O. Auciello and J. A. Carlisle, J. Appl. Phys. Vol 96 pg 2232 (2004)

55. P. E. Pehrsson , F. G. Celii, and J.E. Butler, *Diamond Films and Coating, Development, Prooperties, and Applications*, R. F. Davis, Noyes Publications, Park Ridge, New Jersey, (1993) 68

56. A. Sawabe, T. Inuzuka , *Thin Solid Films* 137 (1986) 89

57. K. Suzuki, A. Sawabe, H. Yasuda, T. Inuzuka, *Appl. Phys. Lett.* 50 1987 728

58. B. Singh, O. Mesker, A. W. Levine, Y. Arie, *Growth of Polycrystalline Diamond Particles and Films by Hot filament chemical vapor deposition.* Report CN-5300, David Sarnoff Research Center. SRI International Princeton , NJ, 1988

59.   P. A. Denning, D. A. Stevenson, *Proc of the 2ⁿᵈ Int. Conf on New Diamond Sci. and Techn.* Pittsburg PA, MRS 1991 pp 403- 408

60.   C.P. Chang, D.L. Flamm, D. E. Ibbotson, J. A. Mucha , *J Appl. Phys*. 69 (1988) 1744

61.   C. P. Beetz Jr. T.a. Perry, *Hot and Cold Wall Fiament-Assisted Growth of Diamond films, General Motors Research Publication GMR-6093* November 24, 1987, p 1-21

62.   S. Yugo, T. Kimura, H. Kanai, in: S. Saito, O. Fukunaga, M. Yoshiharra (Eds), *Science and Technology of New Diamond*, KTK Scientic Pub., Tokyo, 1990, pp. 119-128

63.   K.K. Hirakuri, M Yoshii, G.F. Friedbacher, M. Grasserbauer, *Diam. Relat. Mater.* 6 (1997) 1031-1035

64.   S. Yugo, T. Kanai, T. Kimura, and T. Muto, *Appl. Phys. Lett*. 58 (10) (1991)

65.   S. Yugo, K. Semoto, N. Nakamura, T. Kimura, H. Nakai, M. Hashimoto, *Diam. Relat. Mater*. 6 (1997)

66.   J. Singh, M. Vellaikal, *J. Appl. Phys* 76 (6) 1993

67.   K. V. Ravi, C. A. Koch, *J. Appl. Phys Lett*. 57 (4) 1990

68.   Z. Feng, K. Komvopoulous, I. G. Brown, D. B. Bogy, *J. Appl. Phys*. 74 (4) 1993

69.   A. A. Morrish, P. E. Pehrsson, *Appl. Phys. Lett*. 59 (4) 1991

70.   P. O. Joffreau, R. Haubner, and B. Lux, int. *J. Hard Mater*., 7 (4) (1988) 186

71.   A. Linlbauer, *Ph.D. Thesis*, TU-Vienna (1991)

72.   B. Lux, and R. Haubner, in *Diamond and Diamon-like Films and Coatings*, ed, R. E. Clausing, L. L. Horton, J. C. Angus and P. Koidl, Pleum Press, New York (1991) 579

73.   M. I. Landstrass, K. V. Ravi, *Appl. Phys. Lett*. 55 975 1989

74.   M. I. Landrass and K. V. Ravi, *Appl. Phys. Lett*. 55, 1391 (1989)

75.   O. A. Williams and R. B. Jackman, *Semicond. Sci. Technol.* 18 S34-S40 (2003)

76.   J. B. Cui, J. Ristein, L. Ley, *Phys. Rev. Lett*. 81 429 (1998)

77. J. Ristein, M. Riedel, F. Maier, B. F. Mantel, M. Stammler and L. Ley, *J. Phys.: Condens. Matter* 13 (2001) 8979-8987

78. F. Maier, M. Riedel, B. Mantel, B. F. Mantel, J. Ristein, and L. Ley, *Phys. Rev. Lett*. 85 (16) 3472

79. J. Ristein, M. Riedel, F. Maier, B. F. Mantel, M. Stammler, and L. Ley, *J. Phys: Condens. Matter* 13 (2001)

80. J. A. Garrido, C. E. Nebel, R. Todt, G. Rosel, M-C. Amann, M. Stutzmann, E. snidero and P. Bergonzo, *Appl. Phys. Lett*. 82 (6) 2003

81. A. Aleksonv, A. Denisenko, U. Spitzberg, T. Jenkins, W. Ebert, E. Kohn, *Diam. Relat. Mater.* 11 382-386 (2002)

82. Y. Einaga, G. S. Kim, S. G. Park, A. Fujishima, *Diam. Relat. Mater*. 10 (2001) 306

83. J. F. Prins, *Diam. Relat. Mater*. 4 580 (1995)

84. A. Hatta, S. Sonoda, T. Ito, *Diam. Relat. Mater*. 8 (1999) 1470-1475

85. H. Kiyota, E. Matsushima, K. Sato, *Diam. Relat. Mater*. 6 (1997) 1753

86. H. Okushi, *Diam. Relat. Mater*. 10 (2001) 281-288

87. T. Tsubota, T. Fukui, T. Saito, K. Kusakabe, S. Morooka, H. Maeda, *Diam. Relat. Mater* .9 (2000) 1362-1368

88. C. Levy-Clement, N. A. Ndao, A. Katty, M. Bernard, A. Deneuville, C. Comninellis, Diam. Relat. Mater. 12 2003 606-612

89. S. Haymond, G. T. Babcock, and Greg M. Swain, J. Am. Chem. Soc. 2002 124 10634-10635

90. Y. Show, M. A. Wite, P. Sonthalia, G. M. Swain, *Chem. Mater*., 2003, 15, 879-888

91. S. Bhattacharyya, O. Auciello, J. Birrell, J. A. Carlisle, L. A. Curtiss, A. N. Goyette , D. M. Gruen, A. R. Krauss, J. Schlueter, A. Sumant, P. Zapol, *Appl. Phys. Lett*. 79 (2002) 1441

92. O. A. Williams, S. Curat, J. E. Gerbi, D. M. Gruen and R. B. Jackman, *Appl. Phys. Lett*., vol 85 pg 1680

93.   P. Zapol, M. Sternberg, L.A. Curtiss, T. Frauenhein, D. M. Gruen, *Phys. Rev. B* 65 045403 (2002)

94.   J. Birrell, J. A. Carlisle, O. Auciello , D. M. Gruen, J. M. Gibson , *Appl. Phys. Lett*. 81 (2001) 2232

95.   T. Zimmermann, M. Kubovic, A. Denisenko, K.Janischowsky, O. A. Williams, D. M. Gruen, E. Kohn, *Diam. Relat. Mater*. 14 2005 416

96.   Q. Chen, D. M. Gruen, A. R. Krauss, T. D. Corrigan, M. Witek, and M. Swain, *J. Electro. Chem. Soc.* 148 (1) E44-E51 (2001)

97.   Y. Lin, c. Lin, Y. Chen, Y. Tzeng, P. Tso, I. Lin, *Diam. Relat. Mater*. 13 (2004) 671-678

98.   B. Peng, H. D. Espinosa, *Proc. Of IMECE 2004 ASME International Mechanical Engineering Congress*

99.   A.C. Ferrari, J. Robertson, *Phys. Rev. B* 63 (2001) 121405R